Feature Article

From Franklin to Today: Toward a Molecular Level Understanding of Bonding and Adsorption at the Oil#Water Interface

Cathryn L. McFearin, Daniel K. Beaman, Fred G. Moore, and Geraldine L. Richmond

J. Phys. Chem. C, **Article ASAP**

CENTENNIAL FEATURE ARTICLE

From Franklin to Today: Toward a Molecular Level Understanding of Bonding and Adsorption at the Oil−Water Interface†

Cathryn L. McFearin,‡,|| Daniel K. Beaman,‡,|| Fred G. Moore,§ and Geraldine L. Richmond*,‡

Department of Chemistry, University of Oregon, Eugene, Oregon 97403, and Department of Physics, Whitman College, Walla Walla, Washington 99362

Received: September 15, 2008; Revised Manuscript Received: November 06, 2008

With Benjamin Franklin's oil on water experiments as a historical example, people have long been fascinated with the physical characteristics of the interface between water and an organic liquid and the unique chemistry that can occur at that interface. In this paper, we present our current understanding of the structure, orientation, and bonding characteristics of this fluid and dynamic interfacial region based on the efforts in our laboratory over the past decade and the important research of others in this field. In our studies, in which we have used a combination of surface specific nonlinear vibrational spectroscopy in conjunction with molecular dynamics simulations, we find that a general feature of organic−water interfaces is that of weak bonding interactions between adjacent water molecules and between the water and organic molecules. These weak water−organic interactions, present at all of the interfaces that we have studied, result in significant interfacial structuring and molecular orientation on both sides of the interface. How the structuring of both the interfacial water and organic molecules is dependent on the nature of the organic media is discussed as well as how this interfacial structuring can facilitate molecular and ion transport across the interface. The discussion of the neat organic−water interface is followed by a summary of how this picture is changed with the addition of ions, surfactants, and biomolecules, and how the presence of the organic media plays a role in the adsorption and conformation of adsorbates relative to the vapor−water interface. Examples of recent applications for the oil−water interface to synthesis and future perspectives are discussed as well.

1. Introduction

Its ubiquitous presence in the environment and its paramount importance for the support of the planet's ecosystem gives water a unique position amidst the plethora of molecules that fascinate scientists. This fascination is not a recent phenomenon and thinkers from disparate cultures and schools of thought have studied and puzzled over the behavior of water for many hundreds and thousands of years. Amazing as it may seem, the molecular structure and bonding of bulk water continues to be a hot topic of scientific debate, where fights over water rights, or who is *right* about water, often evoke intense discourse from opposing sides.[1] Emerging from this discussion is the ever growing interest in how water behaves at the terminus of the bulk, where the hydrogen bonding between neighboring water molecules must change to adjust to its new solid, liquid, or gaseous neighbor. How it interacts with its neighboring media is the essence of some of the most important chemical, physical, and biological processes on this planet, many of which we barely understand on a molecular level. Yet advances in our understanding of these interfacial processes have important implications for addressing some of the most pressing scientific issues of today including ion transport, environmental remediation, new materials synthesis and assembly, and environmental chemistry.

Of particular interest to both historical and contemporary investigators have been interfaces between water and a neighboring immiscible liquid or oil. These interfaces have been studied extensively in the last 200 years, and an important historical figure with regard to these investigations in the United States is Benjamin Franklin. Upon witnessing the windblown waves calmed as ships greased with their expelled cooking oil sailed through, he "resolved to make some experiment on the effect of oil on water" when opportunity next arose.[2] In fact Franklin took with him a vial of oil in his cane when going to the country, so as to repeat the experiment in order to further advance his understanding of the impact of oils on the surface of lakes or oceans. The spreading of the oil upon the water's surface fascinated Franklin, and his letters regarding the phenomenon provide accounts that can be enjoyed even centuries later. Fortunately for those living near the lake, and scientific progress, such experiments have now moved into the laboratory. While Franklin and his contemporaries likely did not have the conceptual underpinnings or vocabulary to think in detailed terms of hydrophobic layers, miscibility, diffusion, or interfacial roughness, it is humbling to consider that the sorts

† 2008 marked the Centennial of the American Chemical Society's Division of Physical Chemistry. To celebrate and to highlight the field of physical chemistry from both historical and future perspectives, *The Journal of Physical Chemistry* is publishing a special series of Centennial Feature Articles. These articles are invited contributions from current and former officers and members of the Physical Chemistry Division Executive Committee and from *J. Phys. Chem.* Senior Editors.

* To whom correspondence should be addressed. E-mail: richmond@uoregon.edu. Phone: 541-346-4635. Fax: 541-346-5859.

‡ University of Oregon.

§ Whitman College.

|| Shared first authorship.

10.1021/jp808212m CCC: $40.75

Cathryn L. McFearin received her B.S. in chemistry from Pepperdine University in Malibu, California in 2002. She is currently finishing her Ph.D. research at the University of Oregon under Geraldine Richmond. The focus of this research is on the structure and interactions of interfacial water molecules at liquid−liquid interfaces utilizing vibrational sum-frequency spectroscopy.

Daniel K. Beaman received his B.S. in chemistry from California Polytechnic State University, San Luis Obispo in 2002. He is currently working on his Ph.D. under Geraldine Richmond at the University of Oregon. His research involves surface specific experiments to gain insight into the interactions of surfactant and biological head groups at buried interfaces.

Fred G. Moore received B.A. degrees in mathematics and physics from Lewis & Clark College in 1983 and a Ph.D. in Applied Physics from the Oregon Graduate Center in 1989. After two years as a National Research Council Postdoctoral fellow at the Naval Research Laboratory, he joined the faculty of Whitman College in 1991 and is now Professor & Chair of Physics. His research interests relate to understanding inhomogeneous systems by applying spectroscopic and modeling techniques.

Geraldine L. Richmond is the Richard M. and Patricia H. Noyes Professor of Chemistry at the University of Oregon. Degrees include a B.S. (1976) at Kansas State University and a Ph.D. (1980) at the University of California, Berkeley with George Pimentel. Richmond began her academic career at Bryn Mawr College, moving to University of Oregon in 1985. Her research using laser induced luminescence, nonlinear laser spectroscopy, and computational methods has focused on understanding the chemistry and physics that occurs at complex interfaces that have relevance to important problems in energy production, environmental remediation, atmospheric chemistry, and biomolecular surfaces. Richmond's studies of solid/liquid interfaces include elucidating the factors contributing to photoinduced carrier dynamics at semiconductor/liquid junctions, determining the electronic and chemical properties of these interfaces that contribute to surface passivation and corrosion, measuring the surface morphology and electronic structure for metal and semiconductor/liquid junctions, and examining the molecular structure and dynamics of monolayer assembly at mineral−water interfaces. Her most recent liquid−liquid (the focus of this review) and vapor−water studies have focused on adsorption processes involving gases, ions, acids, surfactants, and biomolecules at these interfaces and the variation of the nature of hydrogen bonding between surface water molecules in these diverse and adsorptive environments.

of "big picture" questions they were asking then are still actively debated and investigated today.

From a modern day perspective, the focus is on understanding the molecular level detail and behavior of water in the vicinity of the oil, or more generally, at a hydrophobic surface. The seminal work by Pratt and Chandler[3] and more recent work by Chandler's group[4,5] focus on the theoretical aspects of these hydrophobic interactions. There are also many other valuable theoretical perspectives that have described water adjacent to a hydrophobic surface and the crossover from a small to a large length scale in the description of the behavior.[4−21] We would also like to note here that "surface" is loosely defined. One might envision a flat two-dimensional expanse, but the surface may well be anything but flat as Tanford points out when reviewing the learning curve that protein chemists faced when confronted with the reality of hydrophobic effects.[22]

It is the fascinating and still elusive properties of this unique interface that has inspired our efforts in this area. In this article we provide a molecular level perspective of the evolution of this field of study with an emphasis on advances made in the past decade. This snapshot of our understanding of the chemical and physical properties of a variety of liquid interfaces will draw on recent experimental and computational studies from our laboratory as well as integrate discoveries and insights from the research of others. Because the nature of this article is more reflective than comprehensive, we urge readers seeking a greater depth of understanding to utilize the primary works we cite.

An additional and exciting aspect of this article is that it provides the opportunity to reflect broadly on how the emergent understanding and future advances of oil−water interfacial systems might contribute to developing areas of science and technology. We invite and welcome others to reflect, as we have done, on how this seemingly unimportant but actually ubiquitous liquid−liquid interface plays a role in their life and scientific thinking.

2. Historical Perspective

Interestingly, it was almost a century after Franklin conducted his oil on water experiments that the thickness of the oil layer was calculated by Lord Rayleigh.[2] Between the time of Franklin and that of Rayleigh, scientists had developed the knowledge and vocabulary to be able to talk about, think about, and work quantitatively with the concept of a layer's thickness but were struggling with the notion of "a molecule". With this as the milieu, there must have been questions about the nature of the transition from the water-side of the layer to the oil-side of the layer. Even in Franklin's time, as engineered flat surfaces of metal and glass became ever more common, people must have pondered the hidden ("buried" in more modern terminology) junction between oil and water. Was it smooth or rough, regular or uneven? However, likely missing from the paradigm view before the turn of the 20th century was any appreciation or sense of the importance of the molecular nature of the system's constituents. Indeed it was only shortly before Rayleigh's work that the composition of water as being H_2O was accepted and that chemists began to fight through the atom/molecule debate.[23]

Through the middle of the 20th century, substantial progress was made in understanding how to exploit the valuable properties of oil−water interfaces. Historically as well as currently, electrochemists have made use of a variety of aqueous interfaces, which are commonly referred to as the interface between two immiscible electrolyte solutions (ITIES).[24,25] The interface between 1,2-dichloroethane and water is a common example for study due to its relatively large polarizable region. Also at this time, polymer chemists made use of the oil−water interface to support the synthesis of materials. The polymerization of nylon from its monomers adsorbed at the interface between an aqueous solution and hexane is the most common.[26] This interfacial reaction is frequently used as a demonstration in introductory chemistry courses as an example of heterogeneous polymerization processes. A quick Internet search for "nylon synthesis" even returns a number of videos capturing the reaction.

More recently biochemists and a variety of theorists have turned to oil−water interfaces as idealized model systems.[27−32] It is humbling to note that some consider these surfaces to be simple and idealized compared to more complex hydrophobic surfaces such as the membrane and cell surfaces that are of interest to them. For many, understanding the detailed molecular behavior of water adjacent to much simpler hydrophobic media, and the response of this interface to the presence of simple ions, acids, and surfactants is challenging enough with many unresolved questions that underpin the behavior of more complex systems that others study.

As instrumentation and the science it enables progressed through the midpart of the 20th century, there was an ever increasing appreciation of the remarkable range of phenomena and behaviors that aqueous interfaces exhibit. With advances in spectroscopy and surface specific techniques through the 1960s and 1970s, the ability to not just appreciate but document the molecular nature of aqueous interfaces began to develop. Since the mid 1980s and the pioneering work by Shen developing vibrational sum frequency spectroscopy (VSFS)[33]

as well as development of second harmonic generation (SHG),[34−38] our group has been applying and contributing to the development of these nonlinear optical methods to explore the behavior of molecules at the interface between water and different organic liquids. Parallel to these advances in nonlinear optical spectroscopy have been advances in X-ray scattering pioneered by Schlossman[39−46] as well as neutron reflectivity[45,47−49] and other more recently developed methods.[50,51] What has emerged from our studies and those employing X-ray techniques is not the placid "stilled surface" that Benjamin Franklin may have anticipated. Rather, the environment at a buried aqueous interface is exceptionally dynamic, awash with molecules experiencing a constellation of bonding environments and sensitive to many conditions. The addition of ions or surfactants causes other behaviors to manifest themselves. It is these ion and adsorbate containing interfaces, which have proven so useful in technological applications to date and that hold much promise for continuing advances.

Coincident with these experimental advances have been the expanding capabilities for using different theoretical methods to describe, predict, and model molecular behavior at liquid−liquid interfaces.[6,52−54] As described in this review, our research effort has greatly benefited from these theoretical advances. These recently developed theoretical techniques and computational models are applied to the specific systems studied in the laboratory resulting in calculations that are directly comparable to experimental data. When good correlation with experimental data is achieved, we can then turn to these calculations to extract a wealth of information about interfacial structure and bonding, resulting in a much deeper and more rigorous understanding of these interfaces than one can derive from a single experimental or theoretical pathway alone.

Our developing understanding, particularly with this combined experimental and computational approach, clearly shows that the appropriate place to begin thinking about interfacial roughness, sharpness, and thickness is at the molecular level where water molecules and oil molecules can venture far across what might nominally be considered the interface. Having foreshadowed some of the conclusions that we have reached, we now return to the beginning where Benjamin Franklin likely thought himself working as he poured his cruet of oil on a pond's surface: the neat oil−water interface.

3. The Neat Oil−Water Interface

This deceptively simple interface, comprised of only two immiscible liquids, is an abundant source of information regarding water next to a hydrophobic surface. The contributions from our laboratory toward the understanding of the fundamental interactions present at an oil−water interface have come from a powerful combination of experimental and computational methods. The questions that we have sought to answer in these studies of the neat oil−water interface are simultaneously simple and complex; simple in concept yet complex when all variables that control the interfacial behavior are brought into play. These questions include: What types of hydrogen bonding interactions between interfacial water molecules are most prevalent at this interface? How does the nonaqueous liquid affect the water bonding behavior, if at all? Is there such a thing as a truly hydrophobic liquid given that all molecules are polarizable to some degree? What are the dimensions of the interfacial region? Does the interface consist of a sharp transition from one liquid to the other or does mixing occur? How might these properties vary with the properties of the nonaqueous liquid? Are there any structural aspects of the oil−water interface that might facilitate molecular or ion transport from one phase to the other?

As mentioned above, the experimental portion of our investigations of the oil−water interface utilize VSFS. In these experiments, a laser beam with a fixed visible frequency is overlapped both spatially and temporally with a tunable infrared (IR) beam at the oil−water interface. A resulting coherent beam at the sum of these two frequencies, $\omega_{SF} = \omega_{vis} + \omega_{IR}$, is then generated. This beam ω_{SF} is only generated by those molecules or collection of molecules that are not centrosymmetric such as the thin interfacial region that possesses an average net molecular orientation. This results in no significant contribution to VSFS signal from the bulk liquid molecules leading to inherent interface specificity. The coherent nature of VSFS results in each resonance having an associated phase that can provide information regarding orientation of the molecules at the interface. Choice of beam polarizations can also provide information about how the molecules are structured. All the spectra presented in this section, both experimental and calculated, use the ssp (s = SF, s = visible, p = IR) polarization scheme, which probes those oscillators with a component of their transition dipole perpendicular to the interface. The experiments are conducted in a total internal reflection geometry to maximize the amount of VSF intensity detected. Details regarding the VSFS background[55−59] and experimental apparatus[60−63] can be found in the references cited.

Once a VSF spectrum is obtained, analysis and assignment of spectral features provides many challenges due to the homogeneous and inhomogeneous broadening of peaks and the more complicated nature of the VSFS response relative to linear spectroscopies like IR and Raman. As in linear vibrational spectroscopies, the frequency and breadth of a VSF spectral peak reveals the nature of the bonding environment being probed. However, in addition the phases associated with the peaks can result in constructive or destructive interference and hence more complex lineshapes. A number of different approaches have been used to best extract the molecular level details that the spectra provide including spectral fitting using a routine developed by Bain[64] that takes into account many of the variables that contribute to VSFS peaks such as amplitude, peak width, frequency, and phase. The curve fitting routines, or related VSFS studies using phase-sensitive measurements,[65] provide mechanisms for identifying spectral features. Curve fitting can assist in the analysis of water spectra, particularly when used in conjunction with isotopic dilution experiments that produce a simpler system of primarily HOD in D_2O.[66] This minimizes the inter and intramolecular coupling between water molecules resulting in spectra that are easier to analyze. However, accurate assignment of spectral features to specific water bonded species becomes more difficult when inter and intramolecular coupling is present. This task is made even more challenging by the interferences between adjacent resonant modes of each type of OH oscillator as a result of the coherent nature of this nonlinear spectroscopy. As a consequence of the complex nature of these interactions and in light of the availability of powerful molecular dynamics (MD) simulation packages, we have recently found a combined VSFS-MD approach to be a valuable way to understand interfacial interactions and interpret spectral features. Examples of this approach are described in the sections that follow.

The CCl_4−water interface was the first oil−water system to be investigated by the Richmond group using VSFS.[63,67] The spectrum obtained using ssp polarization is shown in Figure 1 and will be used to describe spectral features that are found to be common to other liquid−liquid systems examined by VSFS. The spectra correspond to water OH stretch modes that are

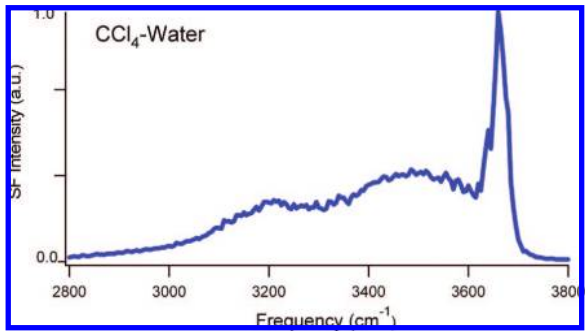

Figure 1. VSF experimental spectrum of the CCl_4−water interface in the ssp polarization scheme.

highly sensitive in frequency and intensity to the degree of hydrogen bonding to other molecules.[68] For the CCl_4−water interface, water is found to be highly oriented as evidenced in part by the presence of the free OH peak near 3700 cm^{-1}. This peak corresponds to the uncoupled OH stretch mode of water molecules that "straddle" the interface, with one OH (the "free OH") oriented into the CCl_4 phase and the companion bond into the aqueous phase. These straddling water molecules tend to reside at the topmost interfacial layer. We have found the free OH frequency to be an indicator of the degree of weak water-organic interaction present at these interfaces.[69]

The companion OH oscillators on those straddling water molecules that are not pointing into the organic phase are necessarily oriented toward the aqueous phase where they are capable of hydrogen bonding with other water molecules. These weakly bound water molecules present in this top region of the interface are largely responsible for the broader peak seen in the spectrum in Figure 1 near 3500 cm^{-1}. Their presence was derived initially from isotopic dilution experiments that measured the spectrum of primarily interfacial HOD water molecules.[63] Because these OH oscillators can act as hydrogen bond donors to other water molecules, the peak is referred to as the "donor OH" peak. This initial interpretation based on the isotopic dilution experiments is consistent with the MD simulations to be discussed later.

The interfacial region also has water molecules that are more tightly hydrogen bound than those described above. They form a network with a greater number of hydrogen bonds to neighboring water molecules that are also stronger in nature. Their spectral contributions appear in the lower frequency region below ≈3400 cm^{-1}. This is the spectral region where the contributing water molecules show more sensitivity to effects that occur deeper in the interfacial region.[70] From these early experimental observations, we concluded that water molecules contributing to this spectral region mainly reside deeper in the interfacial region in comparison to the free OH and donor OH, which have weaker bonding character. The structure of molecules in the spectral region around 3200 cm^{-1} is commonly referred, in a simplistic manner, to water molecules with tetrahedral bonding due to the similar vibrational spectral peaks found in bulk water. In reality, intensity in this region as well as throughout most of the OH stretch region arises from collections of more (less) coordinated or bonded water molecules depending on whether the peaks are at lower (higher) frequencies. In addition, collective effects can also be contributing in these spectral regions as recently noted for the air−water interface.[71,72] The specific types of bonded water species that are contributing to the VSF spectrum and the interfacial depth of these species as determined by MD will follow.

The CCl_4−water spectrum shows similarity in structure to the resonant portion of the air−water spectrum also previously studied by our group.[66] One main difference is the peak frequency value of the free OH mode for the two systems. For the CCl_4−water interface the free OH is at 3669 cm^{-1} versus 3705 cm^{-1} for air−water. This red shift results from the interaction, however small, between the OH of the straddling water molecules with the CCl_4 phase even though it is composed of molecules with no dipole moment making it a highly hydrophobic liquid. The frequency and peak width of the free OH mode are valuable parameters for experimentally judging the extent of interaction between water and the oil under investigation. This will be discussed further for the other more polar oils studied.

From these early experiments we have gained considerable insight into the general nature of the oil−water interface. The interface is obviously relatively sharp with considerable molecular orientation of interfacial water molecules. The VSF spectrum is dominated by weakly bonded water species, specifically the free OH and its companion modes. From spectral fits of the CCl_4−water VSF spectrum, we also find small concentrations of "water monomers" in the interfacial region that are oriented with their hydrogens toward the CCl_4 phase.[63] The peak frequencies of these monomers, in addition to the free OH frequency, show that a weak interaction exists between water and CCl_4 in the interfacial region. Coincident with our early experiments in this area in which we relied on curve fitting routines to give us a general picture of contributing water species, we began conducting MD simulations to compare with our experiments and to shift our thinking to a more comprehensive view of the types of water bonded species that could be contributing to the spectrum. What we gained from these simulations was an expanded appreciation for the need to move our interpretation toward thinking about interfacial water as a continuum of different types of water bonded species rather than a few clearly defined species with specific bonding geometries.

These simulations conducted initially by Brown et al.[73] and later by Walker et al.[74−77] calculate VSF spectra using an approach originally developed by Morita and Hynes.[54] In this technique, snapshots of the water molecule coordinates are recorded at periodic intervals in the simulation, along with the forces acting on each atom using the AMBER molecular dynamics package.[78] The coordinate information is used to project molecular hyperpolarizability tensor elements into the laboratory frame, providing the amplitude of the VSFS response. The force information is used to determine the frequency of the stretching modes. Together, this information gives a calculated VSF spectrum that is directly comparable with experimental results. The density profiles of different interfacial water species, their orientation, and bonding characteristics can then be examined. The naming scheme used for identifying and following differently bonded species is shown in Figure 2. When a molecule is identified with an "O" designation, it means that it is bonded to another water molecule through its lone pair (often referred to as a hydrogen acceptor bond). If it is labeled with an "H", hydrogen bonding to an adjacent water molecule is through that hydrogen (often referred to as a hydrogen donor bond). A molecule labeled as OHH would then be bonded to three adjacent water molecules through its two hydrogens and one of its oxygen lone pairs. For ease of discussion, the different water species to be discussed are organized into four groups. Those labeled as water monomers have the weakest bonding interactions and include those that are either nonbonded or bond only through one (O) or both (OO) lone pairs. The free OH and donor OH containing molecules have one bonded and one nonbonded hydrogen. Since these two OH bonds are energeti-

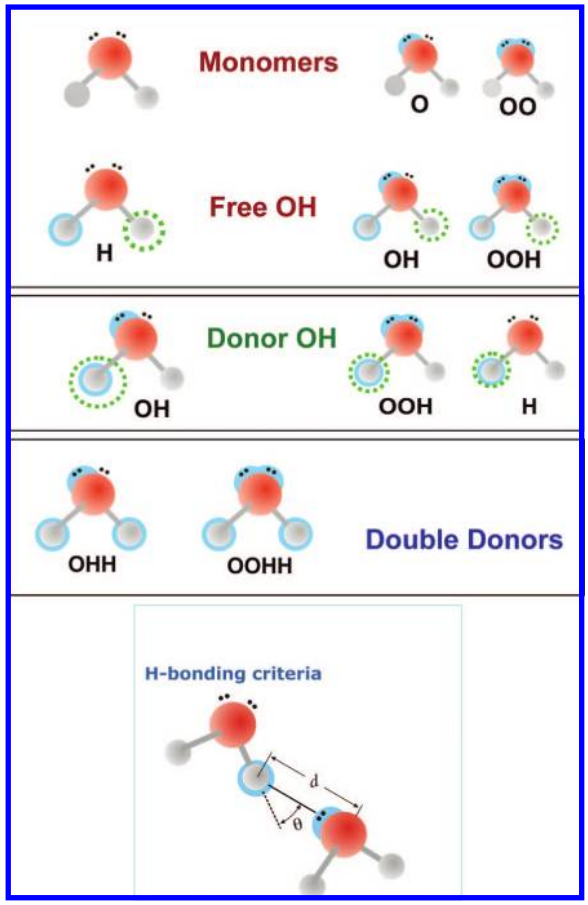

Figure 2. (top) Labeling scheme for the different water bonded species found in the computational VSF spectra. The blue shading indicates hydrogen bonding to another water molecule. Green dotted circles indicate that a hydrogen atom is part of a "free OH" oscillator. (bottom) Angle and distance criteria used to determine if water molecules are hydrogen bonded for the present MD simulations. Adapted from ref 77.

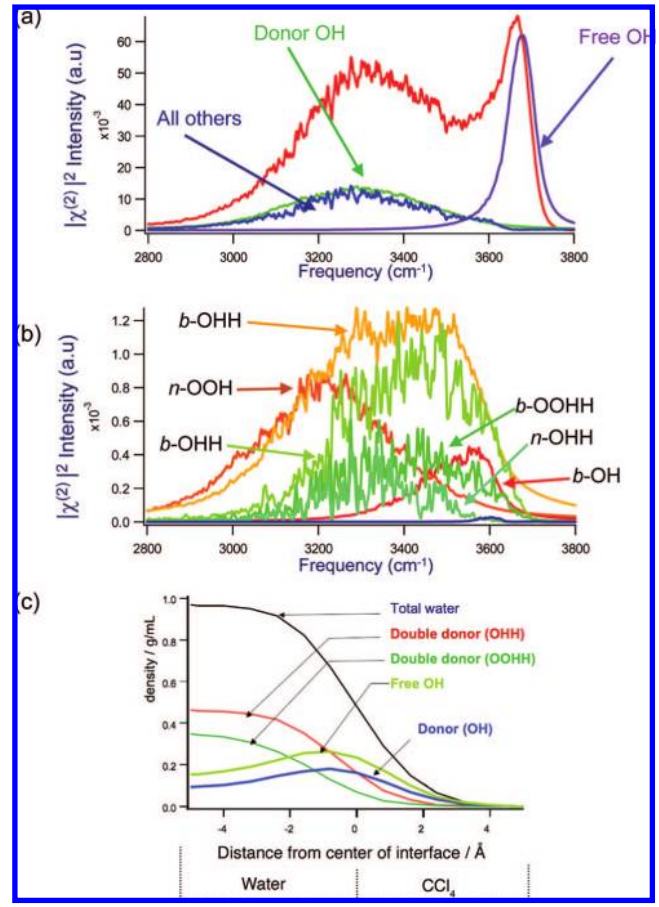

Figure 3. (a) Computational ssp VSF spectrum of the CCl_4−water interface with contributions from the most intense OH stretch modes. Red is the total spectrum; purple is the total free OH, green is the *n*-OH-bonded donor OH; blue is all other modes combined. (b) Computational ssp VSF spectral contributions to the CCl_4−water interface from the next mode intense set of OH stretch modes (blue trace in a). Orange is the *b*-OOH-bonded; dark orange is the *n*-OOH-bonded; light green is the *b*OHH-bonded; green is the *b*-OOHH-bonded; aquamarine is the *n*-OHH-bonded; red is the *b*-OH-bonded; dark blue is the OO-bonded. (c) Density profiles for the dominant water species within the CCl_4−water interfacial region. Adapted from ref 75.

cally uncoupled, we will discuss their spectral contributions separately as free OH modes and donor OH modes.

Each mode as shown can act to different degrees as electron donors. The strongest bonded water molecules are those that bond through both hydrogen atoms and at least one oxygen lone pair (HHO or OOHH). The bottom portion of Figure 2 shows how the distance and angle requirements are specified in order to designate water molecules as being hydrogen bonded. If their intermolecular OH separation was ≤2.5 Å and the corresponding bond angle was ≤30° the two water molecules were considered hydrogen bonded. Situations that satisfied this condition were considered "normal" hydrogen bonds and are designated with an *n*. However there are also contributions to the VSF spectra from interactions that do not satisfy the angle criteria, which are designated "broken" hydrogen bonds and are labeled with a *b*. For example, a molecule designated as an *n*-OH bonded mode consists of a single proton donor and a single proton acceptor through the H and O respectively thus leaving the other OH as an uncoupled oscillator (free OH). This example also meets the angle and distance criteria for intermolecular hydrogen bonding.

The results of the calculations for the CCl_4−water interface are shown in Figure 3.[75] Figure 3a reveals a computational VSF spectrum in reasonably good agreement with experiment (Figure 1). In addition to the total VSF spectrum, spectral deconvolution allows the different water species' contributions to the spectrum to also be shown. The total free OH mode is found at 3670 cm^{-1}, in good agreement with the experimental value determined from spectral fitting.[63] The types of water molecules making the most spectral contribution in the 3000−3600 cm^{-1} spectral region peak are the *n*-OH bonded donor OH modes, again in good agreement with spectral assignments from experiment. Its contribution is broad, reflecting the breadth of interactions that it has with neighboring water molecules. The blue trace in Figure 3a represents all of the remaining water bonded species that contribute to the spectrum. Figure 3b shows the intensities of the most significant species that contribute to this blue trace in Figure 3a. Water molecules with OOH and OHH bonding are the largest contributors. Smaller contributions originate from water molecules with *b*-OOHH and *b*-OH modes. All of these contributing modes are also quite broad in nature and there is a large degree of overlap between them. This exemplifies the importance of these calculations in demonstrating the spectral breadth that these types of modes encompass and their relative contributions, supporting the need for interpretation of VSF spectra to move to a more sophisticated picture of the breadth of interactions occurring at room temperature for these liquid systems.

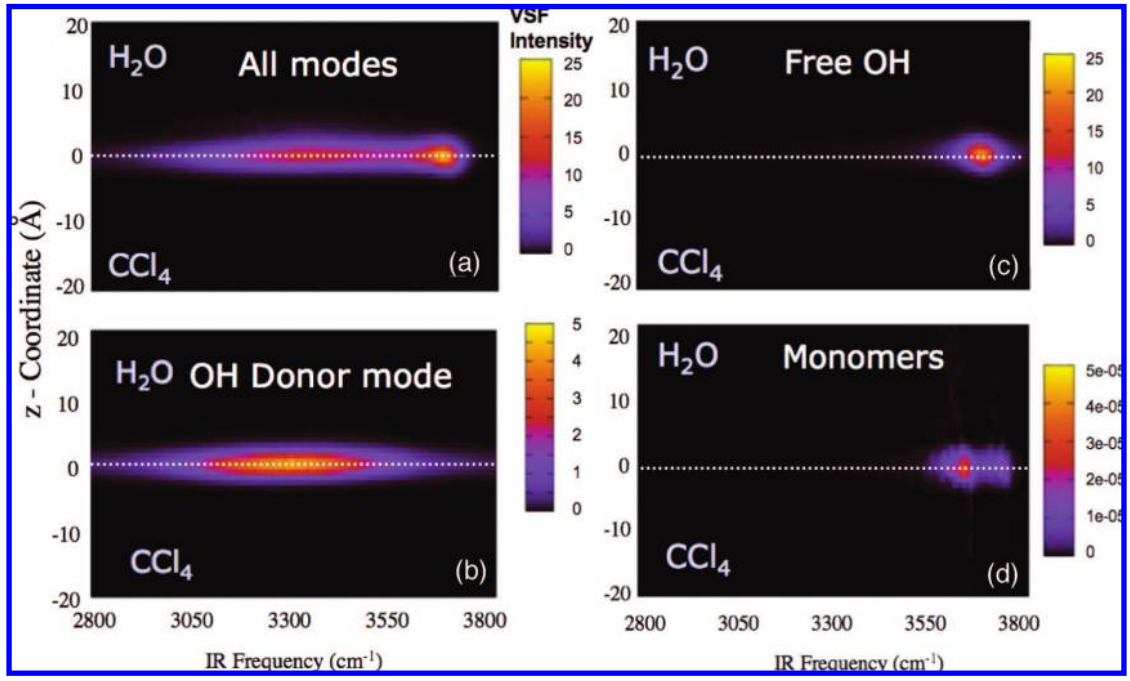

Figure 4. Spectral profiles for the CCl_4−water interface in ssp showing computational VSF intensity as functions of both interfacial depth (*y* axis) and frequency (*x* axis) for all contributing water modes (a), the donor OH modes (b), the total free OH modes (c), and the water monomer species (d). Adapted from ref 74.

More insight can be garnered from density profiles of the different species at the interface as shown in Figure 3c. These profiles are particularly valuable in locating the water species of highest density relative to the center of the interface. As shown, the donor OH mode and the total free OH contributors have their peak populations closest to the dividing surface. The more strongly bonded species with OOH and OOHH bonding peak deeper in the interfacial region toward the bulk water. These calculations support the overall view obtained from the previously described experimental studies that showed the weakest bonding species to be at the topmost interfacial layer.

Orientation profiles (not shown) for these species were also calculated from the MD simulations. These OH-bonded water molecules possessing free OH and donor OH oscillators clearly show tilt angle preferences for these bonds above and below the interface, respectively. Together this explains the large contribution to the VSF spectrum for the ssp polarization scheme, consistent with the experimentally derived conclusions. Interestingly, for OOH-bonded water molecules both the free OH oscillator and OOH-bonded donor OH oscillator tilt angle distributions differ significantly from their OH-bonded equivalents. The OOH-bonded free OH and OOH-bonded donor OH tilt angle distributions are very broad, with directional preference above the plane of the interface toward the organic phase for *both* OH oscillators in both systems. The fact that both OH oscillators for OOH-bonded water molecules prefer to point toward the organic phase suggests that the main driving force behind their orientation preference at the interface is likely due to the formation of hydrogen bonds to other water molecules through the two lone pairs. Orientational analysis of the two types of double donor water molecules found in the density profiles in Figure 3c show that OHH-bonded molecules tend to orient their OH oscillators almost parallel to the interface with a slight angular preference toward the water phase. The OOHH-bonded molecules also tend to orient their OH oscillators almost parallel to the interface and have slightly broader distributions. Overall these double donor water species have a higher density in the full interfacial region than the free OH and donor OH modes but their orientation, which is largely in the plane of the interface, does not contribute to VSF signal in this polarization scheme.

Further insights into the relative VSF contributions from the different water modes and the breadth of their contributions in the interfacial region can be obtained from more recent MD simulations by Walker et al.[74] Several of these depth profiles for the CCl_4−water interface are shown in Figure 4. On the vertical axis is the interfacial position (*z* coordinate) and values are positive for the water side of the interface and negative for the CCl_4 side of the interface. IR Frequency in cm^{-1} is found on the horizontal axis. The entire VSF spectral profile shown in Figure 4a shows that the peak intensity arises from a relatively narrow region at the CCl_4−water interface with the intensity originating from several distinguishable frequency regions of the spectrum. The OH bonded donor mode makes the most significant contribution to the overall intensity as indicated in Figure 4b. The calculated VSF intensity seen in Figure 4 is governed by molecular anisoptropy, thus the depth profiles are a good indication of interfacial width. The second prominent spectral feature is the free OH at the high frequency end. The spectral profile for this mode alone is shown in Figure 4c and one can see that the intensity distribution is relatively narrow both in frequency and interfacial depth. Another interesting and smaller population of water species is the water monomers. The VSF spectral profile of the water monomers, seen in Figure 4d, shows that they have a small contribution to the overall VSFS intensity. Because the OH oscillators of these molecules are coupled, there is both a symmetric and antisymmetric peak for these molecules seen below and above 3700 cm^{-1}, respectively. This subset of water species plays an important role in the resulting overall spectrum when higher concentrations are present at the interface and will be discussed in further detail below. The calculations of the presence of these water monomers are consistent with our early experimental conclusions described above. These calculations of spectral intensity as a

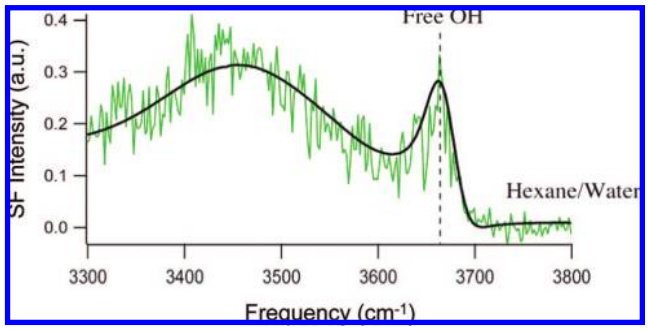

Figure 5. VSF experimental spectrum of the hexane−water interface in the ssp polarization scheme. Adapted from ref 73.

function of interfacial depth are a particularly important addition to information gained by experimental VSFS because one cannot explicitly gain interfacial depth information from it.

Our MD simulations of the CCl_4−water system have benefited significantly from the previous work of others, particularly the pioneering study by Chang and Dang that provided many molecular level details that continue to be referenced.[53] The utilization of polarizable potential models in this study was an especially important step toward using MD to study the oil−water interface as it was the first time to incorporate such polarization effects. Those potential models have been used in other research including the work discussed above. Another interesting aspect of the work by Chang and Dang are results that showed both the water and CCl_4 molecules have significant structural ordering at the interface that was very different than in the bulk. As a result of the orientation of interfacial water molecules, the CCl_4 molecules have a larger induced dipole. The authors predicted this would have implications for ion adsorption and transport at the interface, a topic that has been recently receiving a great deal of attention in the literature and will be discussed later in this paper. Other more recent MD simulations have also been helpful in confirming many of our results.[52,79,80]

We have examined several other oil−water systems with experimental VSFS since the initial investigations of CCl_4−water. Studies of the *n*-alkanes hexane, heptane, and octane at the interface with water revealed comparable spectral features to that of CCl_4−water indicating a similar structural environment for the interfacial water molecules.[73] The results for hexane−water are shown in Figure 5; heptane and octane give a similar response. The free OH peak frequencies from all the alkane−water spectra were determined to be 3674 cm^{-1}, slightly higher than that of the CCl_4−water spectrum. This indicates even less interaction between those OH oscillators in contact with the nonaqueous phase showing hydrocarbons to be somewhat more hydrophobic than the nonpolar CCl_4.

Schlossman and co-workers have also investigated the *n*-alkane−water interface extensively using X-ray reflectivity. The interfacial widths of interfaces between water and *n*-alkanes were calculated from these measurements and compared with widths predicted from capillary wave theory.[43] It was shown previously for hexane−water that the two values agreed,[44] but for the remaining longer alkanes the theory did not match experiment unless contributions from liquid structure (radius of gyration and bulk correlation length for short and long alkanes respectively) were included in the calculation. This discrepancy was also resolved by the same explanation in another study of the *n*-docosane−water interface where the interfacial width determined by experiment disagreed with the capillary wave theory prediction.[46] These X-ray measurements are unique and important because they can experimentally examine the interfacial width of a neat interface, a characteristic of fundamental interest to many researchers.

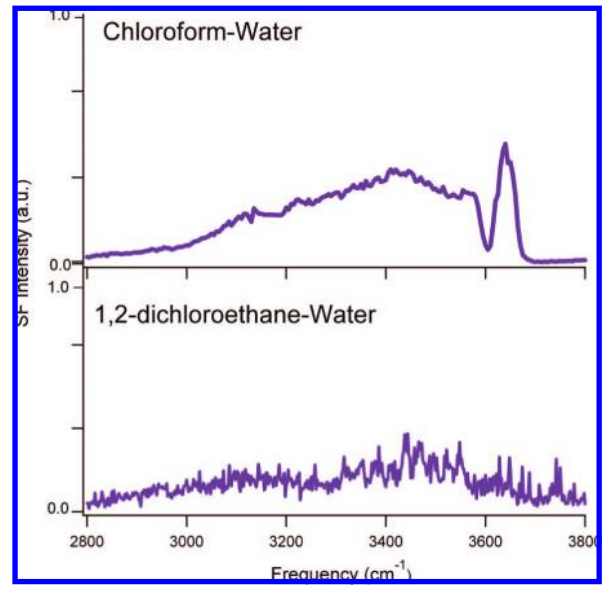

Figure 6. VSF experimental spectra of the chloroform-*d*−water interface (top) and 1,2-dichloroethane−water interface (bottom), both in the ssp polarization scheme.

The CCl_4−water and alkane−water interfaces represent systems of water adjacent to a hydrophobic nonpolar liquid. Another set of VSFS experiments from our laboratory have examined the interface between water and some slightly more polar halocarbons: 1,2-dichloroethane (DCE), dichloromethane (DCM), and chloroform.[62,81] The results of these studies shown in Figure 6 convey the interesting effects of liquids with varying polarity on the behavior of the interfacial water molecules. The chloroform−water spectrum shows a reduction in intensity and red-shift of the free OH peak when compared to the CCl_4−water spectrum (Figure 1). The resulting peak frequency for the free OH of chloroform−water interface is 3645 cm^{-1} attributed to a larger degree of interaction between the two phases than has been observed previously for CCl_4−water and the alkane-water interfaces. In contrast, the DCE-water spectrum shows very little intensity or spectral structure. This trend of decreasing spectral intensity is dependent on the polarity of the liquids. Chloroform has the smallest permanent dipole moment and shows the most spectral structure, more similar to that of CCl_4−water. DCE, with the largest dipole moment in its gauche conformation, shows a spectrum that is largely featureless. DCM (not shown) has a behavior intermediate between chloroform and DCE and also a polarity between both liquids. Qualitatively, these observations imply less water orientation resulting in a less ordered interface for water next to a more polar liquid. This arises because of increased interactions of the interfacial water molecules with these halocarbon molecules because, unlike CCl_4 or the alkanes, they all possess a permanent dipole.

A recent study from our group done by Hore et al. used MD to investigate the overall water orientation at the interface with several hydrophobic phases: halocarbon liquids CCl_4, chloroform, and DCM in addition to vapor.[82] This was done by calculating the order parameters for interfacial water molecules from the simulations of the different interfacial systems. These parameters are a measure of the extent that the water molecules orient with respect to laboratory frame coordinates and are shown in Figure 7 along with a definition of the molecular and

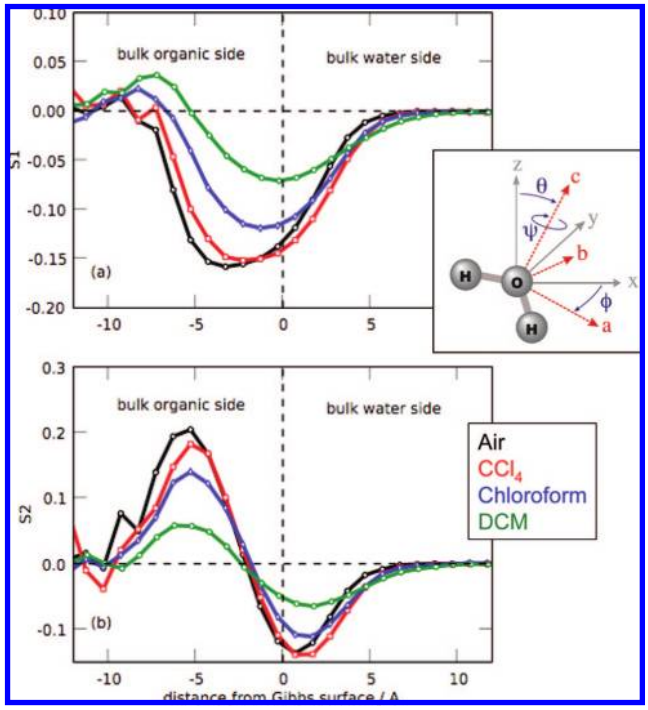

Figure 7. Orientation of water molecules adjacent to four different hydrophobic media: air (black), CCl_4 (red), chloroform (blue), dichloromethane (DCM, green) given by the tilt S_1 (top) and twist S_2 (bottom) order parameters as a function of interfacial depth. A cartoon of a water molecule defines the axes systems used to calculate the order parameters. Adapted from ref 82.

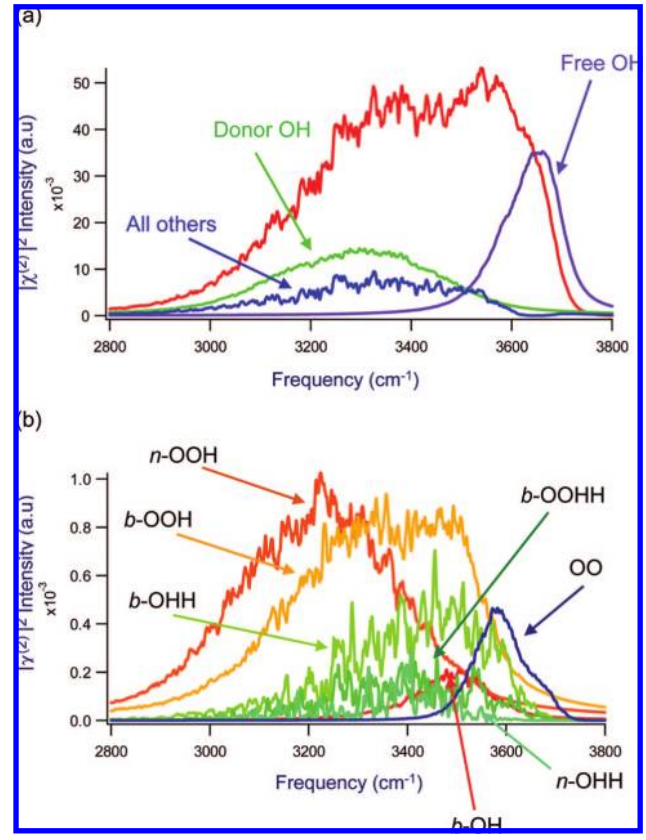

Figure 8. (a) Computational ssp VSF spectra of the DCE−water interface with contributions from the most intense OH stretch modes. Red, total spectrum; purple, total free OH; green, *n*-OH-bonded donor OH; blue, all other modes combined. (b) Computational ssp VSF spectral contributions to the DCE−water interface from the next mode intense set of OH stretch modes. Orange, *b*-OOH-bonded; dark orange, *n*-OOH-bonded; light green, *b*-OHH-bonded; green, *b*-OOHH-bonded; aquamarine, *n*-OHH-bonded; red, *b*-OH-bonded; dark blue, OO-bonded. Adapted from ref 75.

laboratory frame axes. The parameter $S_1 = 0.5\langle 3\cos^2\theta - 1\rangle$ and measures the degree of ordering of the tilt angle θ between the molecular *c*-axis with respect to the interface normal. For a value $S_1 = 1$, the water molecule is aligned with the *c* axis pointing out of the interface. For a value $S_1 = -0.5$, the molecule has its *c*-axis in the plane of the interface. The other order parameter $S_2 = \langle \sin\theta\cos 2\psi\rangle/\langle \sin\theta\rangle$ and conveys the degree that water molecules are twisted by ψ about the *c*-axis. A value of $S_2 = 1$ results in $\phi = 0°$ or 180° and $S_2 = -1$ indicates that $\phi = 90°$ or 270°. If there was no net orientation of the molecules under consideration, both order parameters would have values equal to zero.

Examining the magnitudes of both order parameters in Figure 7 reveals the trend that for liquids with weaker dipole moments (less polar) there is a greater degree of orientation of water molecules near the Gibbs dividing surface. One exception of this is seen for water molecules that have their oxygen atoms directed toward the water phase ($S_1 > 0$) and are found several angstroms into the nonaqueous side of the interface. The two dominant populations shown by the S_2 parameter are the straddling molecules ($S_2 > 0$) found 6 Å into the nonaqueous side of the interface and those with their OH's in the plane of the interface ($S_2 < 0$) found 1 Å into the water side of the interface. An earlier study of water next to apolar liquids by Jedlovszky et al. using Monte Carlo simulations also found the existence of these different populations of water molecules residing in the interface.[79] Both studies show water molecules at all the interfaces studied have significant orientation (nonzero values for the order parameters) for these populations, but again the interfacial systems with the least polar nonaqueous liquid showed the greatest extent of orientation. This study confirms the explanation of the VSFS results described earlier.

As shown in Figure 6, the VSF spectrum of the DCE–water interface shows a significant departure from the other liquid−liquid systems discussed thus far. Because the DCE−water spectrum displayed so little intensity and could not be analyzed using conventional spectral fitting methods, further investigation was warranted in order to better understand the structure of that interface. MD simulations were carried out by Walker et al. for this oil−water system and used to calculate a VSF spectrum to gain more insight into the interfacial water species populations.[75] Figure 8 contains the different contributions to the overall calculated VSF spectrum. Figure 8 reveals that, although not evident in the experimental spectrum, the DCE–water spectrum is composed of similar water species that comprise the CCl_4−water spectrum. The total free OH mode is present at 3650 cm^{-1} (purple trace), which is red-shifted relative to the CCl_4−water free OH. The DCE−water free OH peak is also broader in comparison. These differences in peak characteristics are attributed to stronger dipole interactions present between the water and more polar DCE molecules. The deconvoluted spectrum also shows that *n*-OH bonded donor OH modes are present in substantial population at the interface (green trace) and have the most intensity in the lower energy region of the spectrum. The remaining modes contributing to the spectrum (blue trace) are comprised of OOH and OHH-bonded modes similar to that at CCl_4−water but with less contribution from the *b*-bonded species. These are shown in Figure 8b. Another interesting difference that surfaces when examining the contributions to the spectrum is that there is a significant increase in intensity from the OO-bonded water species and water mono-

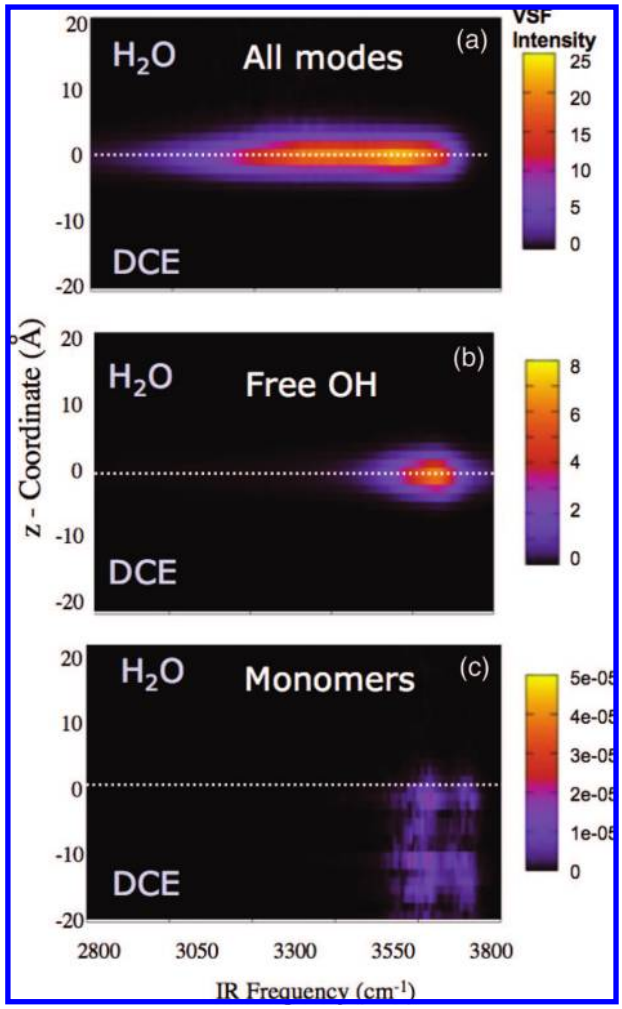

Figure 9. Spectral profiles for the DCE−water interface in ssp showing computational VSF intensity as functions of both interfacial depth (*y* axis) and frequency (*x* axis) for all contributing OH modes (a), only the free OH modes (b), and only the water monomer species (c). Adapted from ref 74.

mers that are oriented at the DCE−water interface. When taken altogether, these subtle but important differences in water species present at the interface can help explain the appearance of the largely featureless DCE−water spectrum in comparison to that of CCl_4−water. Because the free OH for DCE−water is present at a lower peak frequency and broadened due to increased interaction with the DCE phase, destructive interference between the free OH and donor OH modes occurs to a greater extent than at CCl_4−water. This is due to the free and donor OH modes having opposite phases and increased spectral overlap, resulting in less obvious VSFS peaks. The lack of intensity contribution from *b*-bonded species in addition to the increased contribution due to oriented OO-bonded waters and monomers also adds to the effects of interference thereby complicating this region of the spectrum between 3500−3700 cm^{-1} even more. The result is that the VSF spectrum of DCE−water appears to have little spectral structure but upon closer investigation, shows that it has significant water orientation.

To further understand this complex oil−water system, a VSF spectral depth profile study of the DCE−water interface was also performed using MD simulation methods.[74] The results are shown in Figure 9 and reveal how the different water species discussed in the previous paragraph penetrate and orient to a greater degree when in contact with a more polar liquid such as DCE in comparison to CCl_4. Unlike the depth profile for CCl_4−water (Figure 4a) one can see in Figure 9a no distinctive free OH contribution, but rather the intensity is continuous from ≈3200−3700 cm^{-1}. Also the intensity extends depth-wise, further showing the interface to have a broader region of oriented water molecules than CCl_4−water. Said another way, the interface is widened due to the increase in oriented water molecules into both phases. Figure 9b focuses only on the profile of the free OH peak and shows that the mode is quite broad in frequency and depth with a "tailing" into the lower frequency region. This is again attributed to the increased interactions between water and DCE molecules due to the more polar nature of DCE. Also very interesting is the profile for water monomers shown in Figure 9c. It shows that the spectral contribution comes from these water molecules that have penetrated several layers into the DCE phase and possess significant orientation so that they generate VSFS intensity. From these computational efforts, a more complex picture of the interactions between DCE and water emerged than was previously thought. This demonstrates how effective combining experimental and computational methods can be in studying the oil−water interface. Credit should be given to the pioneering MD simulation work done by Benjamin on the DCE−water system.[6] This and other works by Benjamin recognized the DCE−water interface as an important system to use in order to better understand phenomena like charge transport. These studies characterized the DCE−water interface as molecularly sharp but roughened by capillary waves. This analysis provided some of the first information about the molecular level structure and dynamics for this important oil−water system.

Interfacial polarity has also been examined by Walker and co-workers in their work on molecular rulers using another nonlinear optical technique, second harmonic generation (SHG).[37,38] In these studies, originally employed by Eisenthal and co-workers,[83] chromophores with different polar and nonpolar properties are used to probe the same oil−water interface. The SHG intensity is sensitive to how the chromophores are solvated because of changes to their electronic properties. The result is a series of electronic excitation spectra, which reveal that the polarity at an oil−water interface is not necessarily a simple average of the two bulk phases but rather can have different dielectric environments.

Until this point, the main focus of our research has been on the water phase of the oil−water interface. This is partially due to people's fascination with liquid water but also due in part to the complexity of extending both experimental and computational VSFS techniques to examine the oil phase. Recently several MD studies from our group have attempted to fill this gap. One such study by Hore et al. focuses on the orientation profiles of both phases of the DCM−water and chloroform−water interfaces.[84] Expanding upon previous work by Jedlovszky et al.,[79] this study calculates tilt and twist angle order parameters both for water and the halocarbon molecules as a function of depth from the organic side to the aqueous side of the interface. One particularly interesting result from these studies is the visualization of how the molecules in the two phases orient at the interface to maximize the hydrogen bonding interactions between them. Cartoons of the average orientations adopted by the chloroform and DCM molecules in contact with water are shown in Figure 10. The resulting maximum orientation for chloroform results in a slight tilt of the C−H bond coinciding with a large population of water molecules that adopt an in-plane orientation thereby creating an opportunity for hydrogen bonding between the two molecules. The DCM−water case is

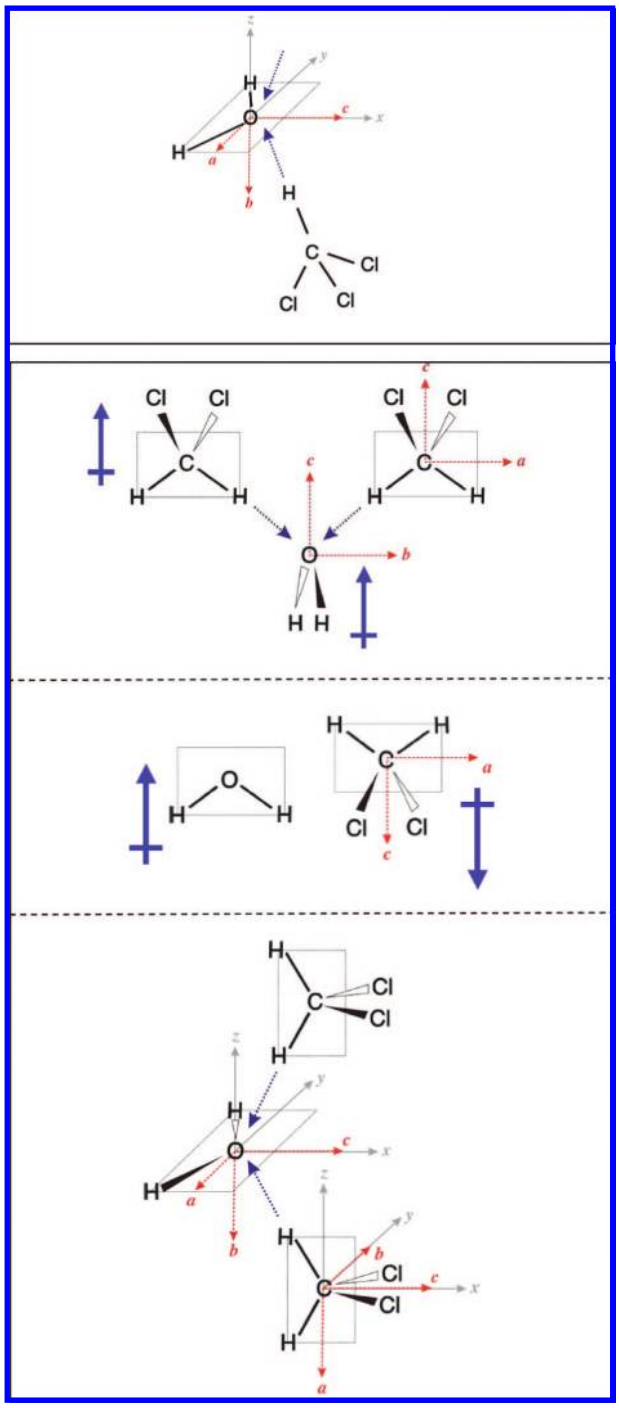

Figure 10. Orientation of water and chloroform molecules adopted at the interface to maximize hydrogen bonding interactions (top). DCM and water predominant orientations at different regions within the interface proceeding from deepest into the DCM phase toward the aqueous phase. Dashed blue arrows indicate hydrogen bonding and solid blue arrows show permanent dipoles of the molecules with the arrows pointing toward the more electronegative molecules or atoms. Adapted from ref 84.

more complicated. As shown in Figure 10, the DCM molecules adopt several different configurations throughout the interfacial region that, when considered with the different water populations present at these depths, result in hydrogen bonding interactions taking place for only a certain subset of these geometries. Although CCl_4 does not have a permanent dipole, its structure at the interface with water has been shown in another study by Hore et al. to also be affected by the overall water orientation.[85]

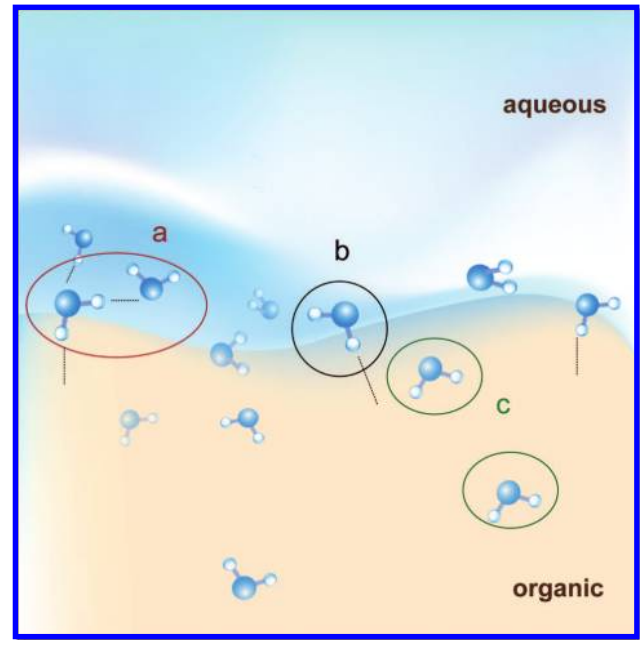

Figure 11. Cartoon of the oil−water interface showing different weakly bound water species that make up the aqueous phase: straddling water molecules that are hydrogen bonded to other water molecules (a), straddling water molecule only interacting with the organic phase (b), water monomers present on the organic side of the interface (c).

In this study, the CCl_4 phase was observed to have a layered structure consisting of corner and face orientations directed toward the bulk water phase. It is thought that this structuring occurs in response to the out-of-plane field created by the highly oriented water molecules at the interface. It is clear that these intermolecular interactions greatly affect the overall molecular structure of the interface and should play a large role in adsorption processes at the oil−water interface.

Through the work discussed above, we have attempted to answer several of the questions outlined at the beginning of this section regarding the structure of the oil−water interface. The conclusions we have settled upon at this time can be summarized in part by considering the physical picture emerging of the structure of the interface shown pictorially in Figure 11. The interfacial region is relatively sharp with both the water and organic molecules highly oriented in nature. Their structure however is integrally related to the polarity and polarizability of the organic liquid present at the interface. The characteristics of the nonaqueous liquids under consideration also largely dictate the degree of water−organic interactions that occur. Interestingly though, all the oil−water interfaces studied, even those where the oil was completely nonpolar (very hydrophobic), showed some degree of interaction between the two phases. In the interfacial region directly between the two liquids, the dividing surface, the water shows the weakest bonding characteristics and the density is the lowest here as well. These water molecules are represented by species a and b in Figure 11, which show straddling waters with different degrees of hydrogen bonding. However, this junction does not necessarily mean there is no mixing occurring. Some number of water molecules (c in Figure 11) still penetrate into the organic phase despite the sharp divide of the interface. Again this is dependent upon the properties of the organic phase.

The wealth of information gathered from the many years of work discussed above demonstrates that the neat oil–water interface is an interesting and quite complex system. When one considers the different properties that the nonaqueous phase can

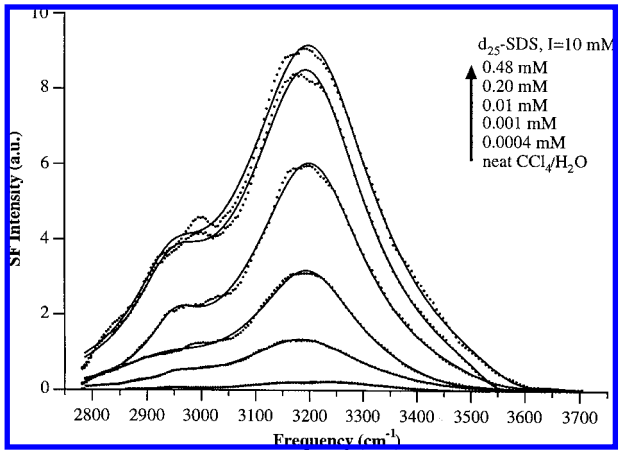

Figure 12. VSF spectra of SDS at the CCl_4−water interface in the ssp polarization scheme. Adapted from ref 86.

have and how that alters the structure of the interfacial region through various orientations and bonding characteristics of the water molecules, it shows how imperative a solid foundation is to fully grasp the subject of the next section.

4. Adsorbates and Ions at the Oil−Water Interface

Having provided a solid foundation on the neat oil–water interface in which a picture of water structure next to a variety of hydrophobic liquids was assembled, we can now turn our attention to the perturbation of the oil−water interface through the addition of ions, surfactants, and biologically relevant molecules. With the addition of these solutes, it is possible to study how the molecular level picture of the neat oil−water interface evolves with respect to the properties of an adsorbed species, as well as to see how the adsorbates orient and pack when placed in this unique interfacial region. For this discussion, adsorbates studied over the past decade are divided into two main groups of study. The first are smaller inorganic ions, and the second are surfactants and biomolecules. For reasons previously discussed, the difficulty in ascertaining information about this interface leaves only a few techniques to study adsorbates at the oil−water interface. As in the previous section, the focus will be on experiments using VSFS, X-ray reflectivity, and MD simulations. This section begins by examining how water structure next to a hydrophobic liquid changes in the presence of ions and charged surfactants, and then moves on to the structure of the adsorbates, delving into their conformation and orientation at the oil−water interface.

When a charge is placed at the oil−water interface, an electrostatic field is produced which reorients the water molecules from their initial neat configuration. Early work by Gragson et al. provides evidence of water restructuring in the presence of the charged surfactant sodium dodecyl sulfate (SDS).[86,87] Results of charged surfactants added to the CCl_4−water interface show a large enhancement in the water peak at 3200 cm^{-1} as seen in Figure 12, which represents the more highly coordinated water molecules in the interfacial region.

In general, an enhancement in VSF signal can either be due to an increase in the orientation of the molecules, or an increase in the number of molecules contributing to the signal. In the case of the SDS work near monolayer coverage, the increase in signal is due to an increase in depth of the sampled interfacial region, as well as increased alignment of the more highly coordinated water molecules within this region. These conclusions are supported by temperature dependent investigations from this same study, which show a decrease in this same low frequency mode as temperature is increased. This is due to the increased thermal energy and randomization of the transition dipole, hence the interfacial region becomes narrowed as fewer molecules are aligned which leads to a decrease in the VSF signal. Berkowitz and co-workers completed MD simulations of SDS at the CCl_4−water interface and their results support the conclusions in which water dipoles align and interfacial depth is increased as the electrostatic field is increased at the interface.[88,89]

The experimental studies by Gragson et al. sampled the overall interfacial water structure in the presence of SDS near monolayer coverage, which includes water molecules in the electrostatic field and in the interfacial region far from the headgroup. Consequently, VSF signal from the water molecules in the double layer region dwarfs the signal from the small number of water molecules solvating the surfactant headgroup. The work of Scatena and Richmond focused on these solvating water molecules in their studies of nanomolar concentrations of deuterated SDS and dodecyltrimethylammonium chloride (DTAC) at the CCl_4−water interface.[90,91] In Figures 13 and 14, the changes to the neat spectrum of CCl_4−water are shown as small concentrations of SDS or DTAC are added. Significant changes in the OH bonded region are found and the free OH is prevalent through the whole low concentration regime. At the highest concentration of 5 mM (the top of Figures 13 and 14), the spectrum has evolved to one similar to that of Figure 12 where the intensity comes largely from the strongest bonded water species. At the low "gas like" concentrations of SDS and DTAC, changes in the OH stretch region are a direct reflection of the water molecules solvating the charged headgroup. One of the most notable features of the low concentration data series of SDS and DTAC is that these solvating water molecules show very weak hydrogen bonding with spectral signatures around 3600 cm^{-1}. As SDS concentration is increased, a notable intensity decrease is seen in this region, whereas with DTAC, an increase in VSF intensity in this region is observed. When these concentration series are fit, there exists a 180° phase difference between the peaks located in the 3600 cm^{-1} region for SDS and DTAC, indicating a 180° phase difference in the orientation of the water dipoles represented by this peak.

Figure 15 is a descriptive picture of solvating water molecules that the authors attribute to these spectral changes where the dipoles of the water align with the field at the interface due to the adsorbate; taking note that the dipoles of water are oppositely aligned for SDS (dipole pointed toward H_2O) and DTAC (dipole pointed toward CCl_4) due to the opposite charge of the head groups, and hence reversed field effects at the interface.

In these early studies of charge effects at the oil−water interface, all of the species were known to adsorb and concentrate their charge at the interface. More recently, there has been a surge in interest in whether small inorganic or molecular ions in an aqueous solution exist in the interfacial region, and if they do, how they alter the properties of the water surface. Although there has been far more work on this topic at the oil−water interface, a few recent studies are beginning to address this issue at oil−water interfaces as described below.

Again, surface specific experimental techniques like VSFS and X-ray reflectivity, as well as MD simulations, have been at the forefront of the evolving picture of ions at the oil−water interface.[92−94] Work utilizing both X-ray reflectivity and MD on tetrabutylammonium salts at the nitrobenzene-water interface showed that common mean field theories such as Gouy−Chapman

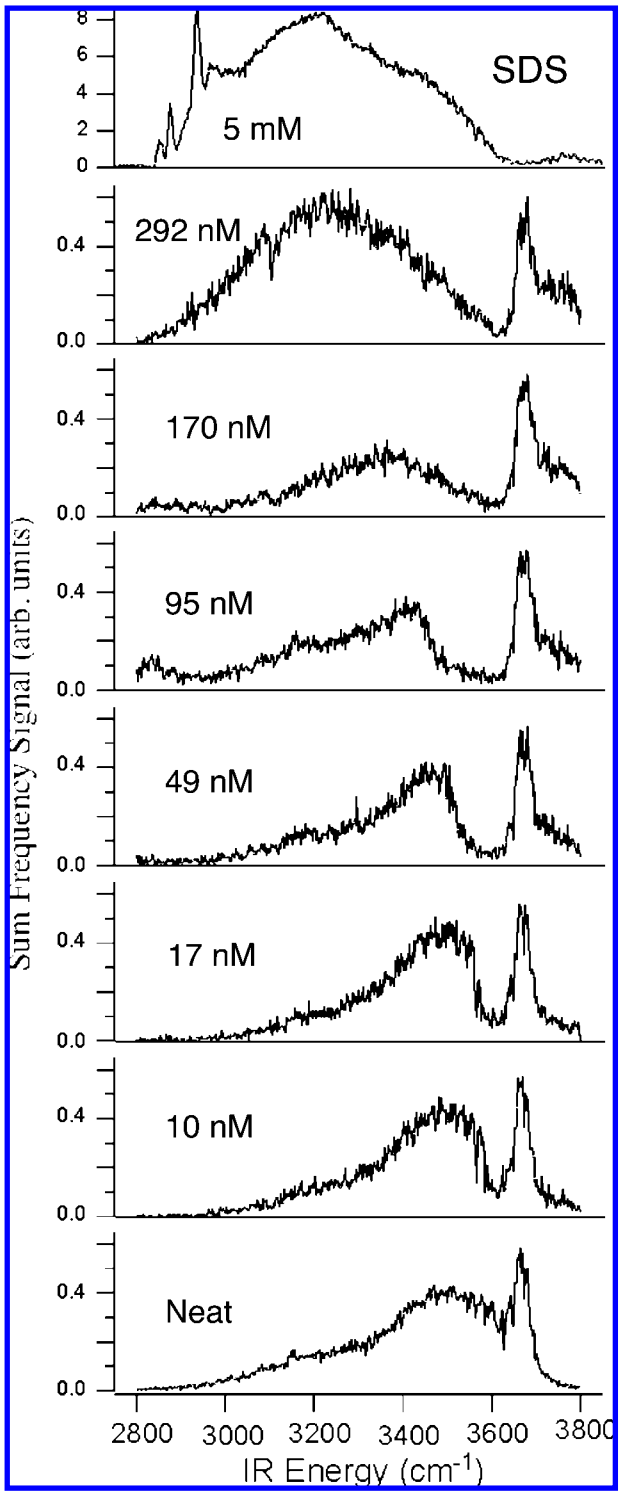

Figure 13. VSFS spectra of d-SDS concentration series at the CCl_4−water interface in the ssp polarization scheme. Adapted from ref 90.

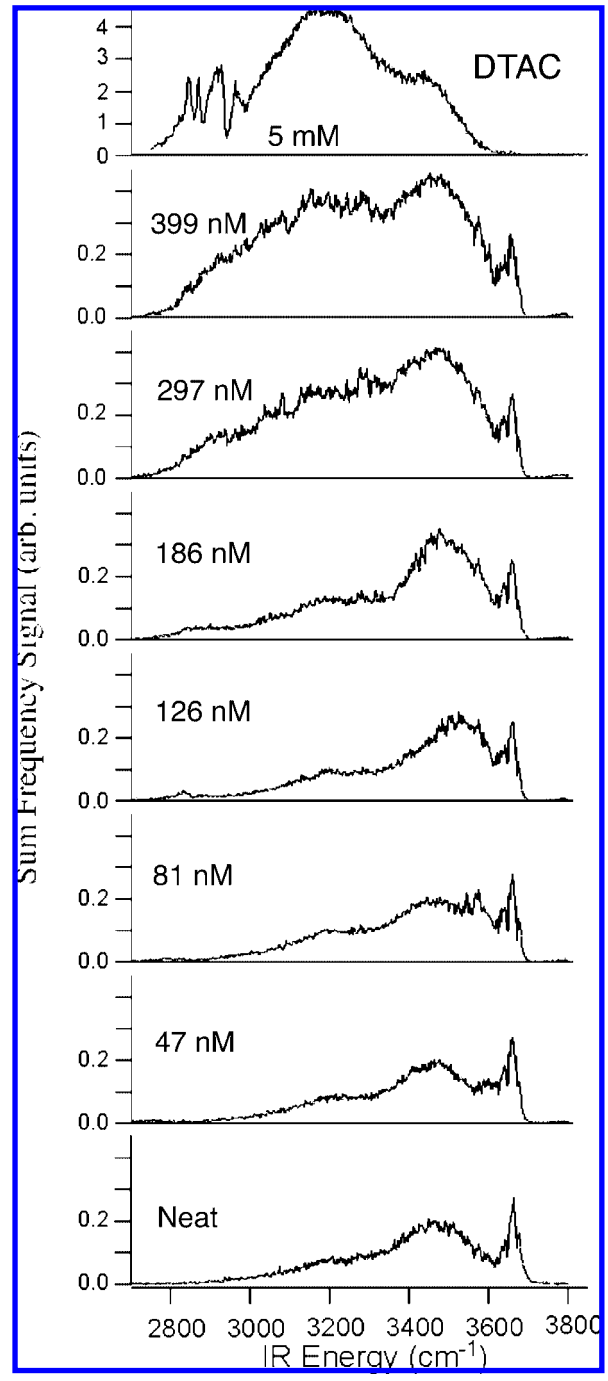

Figure 14. VSFS spectra of d-DTAC nM concentration series at the CCl_4−water interface in the ssp polarization scheme. Adapted from ref 90.

theory give predictions that are not in agreement with experimental measurements.[39,41] This shortcoming was attributed to the inability of the theory to model the molecular scale structure of the liquid solution. The MD results calculated the potential of mean force by taking into account liquid structure through parameters such as ion size and ion−solvent interactions, which were used to predict ion distributions for the experimental situation. These results showed excellent agreement when compared to ion distributions obtained from the X-ray measurements.

Recent works by Wick and Dang have focused on the behavior of small inorganic ions at aqueous interfaces using MD.[95−97] Their work examined molar solutions of halide ions at the CCl_4−water, DCE−water, and air−water interfaces. The results of these calculations support the notion that anions are present at higher concentrations within the interfacial region than in the bulk. However the degree of accumulation at the interface is larger for more polarizable ions like Br^- and I^-. These ions also appear to exhibit higher interfacial concentrations at the air−water interface than at the CCl_4−water interface, with the DCE−water interface showing the lowest concentrations. Cl^- shows similar peak concentrations at both the CCl_4−water interface and the air−water interface. However, unlike the air−water interface, their studies suggest Cl^- extends

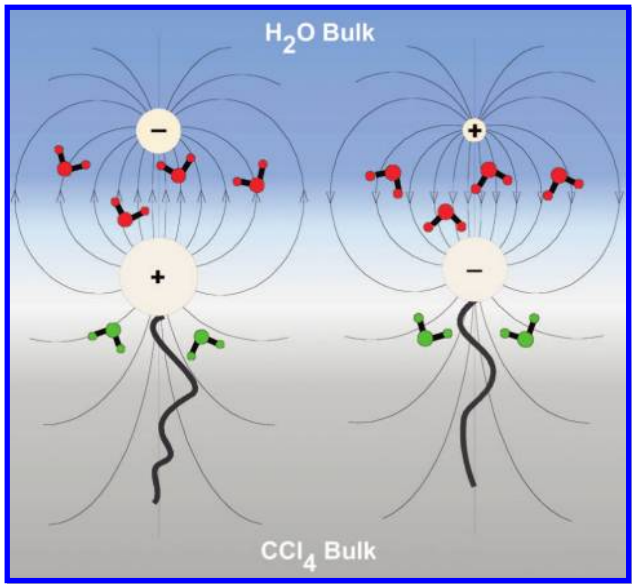

Figure 15. Schematic of how the induced fields from DTAC (left) and SDS (right) orient the water molecules solvating the head groups of the surfactants. Adapted from ref 90.

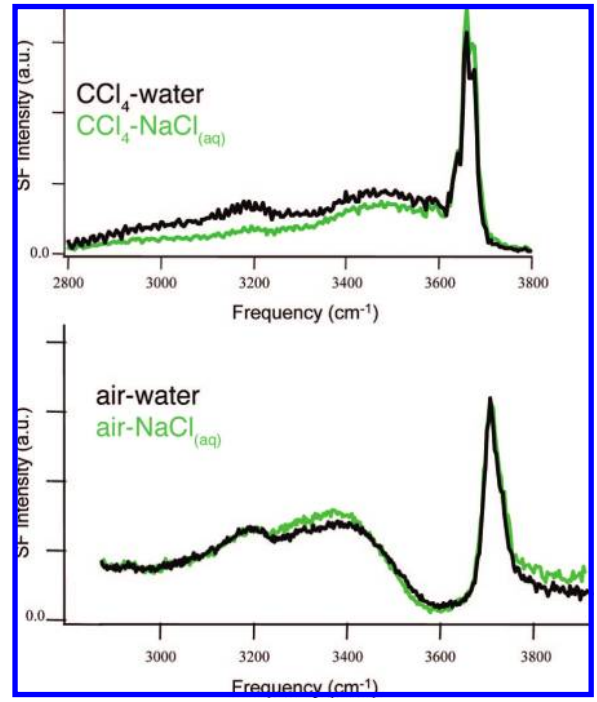

Figure 16. VSF experimental spectra of aqueous molar NaCl solutions at the interface with CCl_4 (top) and air (bottom) shown by the green traces. For comparison, black traces show the neat CCl_4−water and air−water spectra on top and bottom, respectively. Both spectra are in the ssp polarization scheme.

further into the CCl_4 phase, resulting in a larger overall presence of Cl^- at the interface. Interestingly, they find that Cl^- shows no affinity for the DCE-water interface and is in fact repelled from this particular interfacial region. These simulations provide additional evidence that unique interactions take place that are specific to the identity and characteristics of both the ion and oil−water interface under investigation. Further, they show that replacing the vapor phase with an organic liquid can influence the ion behavior and in turn the interfacial water molecules.

In our laboratory, VSFS and MD studies are currently underway to examine the influence of ions at the oil−water interface. Initial studies of molar solutions of NaCl at the CCl_4−water interface show the ions have a significant impact on the interfacial water structure. This is depicted in Figure 16, which displays the VSF spectrum of the CCl_4−$NaCl_{(aq)}$ interface (top) with the air−$NaCl_{(aq)}$ (bottom) spectrum taken from a previous study for comparison.[98] While the neat CCl_4−water and neat air−water VSF spectra share similar features, the presence of the ionic solutions has distinctly different effects on the two different systems. It can be seen in the CCl_4−water spectrum that the intensity below 3500 cm^{-1} decreases with the addition of NaCl, corresponding to the more strongly bonded water molecules that are deeper in the interfacial region. A decrease is also seen between 3500−3600 cm^{-1} in the CCl_4−water spectrum, which corresponds to changes in the topmost layer of interfacial water molecules. This strongly contrasts the air−water spectrum in which the intensity slightly increases in the 3200−3500 cm^{-1} region, but no significant change in intensity is seen between 3500−3600 cm^{-1}. Although the MD studies discussed above show only a small amount of Cl^- enrichment at the CCl_4−water and air−water interfaces, the experiments indicate that Cl^- is present in the interfacial region of CCl_4−water and additionally they penetrate and perturb water in the topmost interfacial region. However, they do not appear to be at a high enough concentration to alter the free OH peak. This further emphasizes the importance of considering the effects the oil phase can have on processes such as ion transport of charged species at the interface. Effects of other ions on the CCl_4−water interface (both cations and anions) are under further investigation and will be the subject of future publications from our group.

The subject of ion specificity at interfaces has also been investigated using VSFS by Cremer and co-workers.[99,100] Although not technically an oil−water interface, the systems probed are ionic solutions adjacent to a hydrophobic phase. The goal of Cremer's studies was to gain a better understanding of how different ions affect both the polymer monolayer adsorbed at the air−water interface and the water structure of the solution subphase. The importance of this system is that it can be viewed as a model for water next to larger biomolecules such as proteins. The ions can then be classified relative to the Hofmeister series, which categorizes salts on their ability to precipitate proteins from solution.[101] The results of this study showed that with just the polymer monolayer present next to a pure water subphase, the VSF spectrum contained only peaks due to the CH moieties from the polymer with very little signal due to interfacial water stretching modes in the 3200−3500 cm^{-1} region. However, as salts were added to the aqueous subphase, the intensity in the OH stretch region increased where the extent of increase was directly related to which anion was present. At a given concentration the anions that were more polarizable (those found on the "chaotropic" end of the Hofmeister series such as SCN^- and I^-) showed the greatest increase of VSF signal in the OH stretching region. This increase in signal was attributed to alignment of interfacial water molecules within the subphase upon addition of charge from the anions.

It is interesting to compare these results to those described above for anions present at the CCl_4−water interface and the air−water interface. As discussed in the previous section, VSF spectra of those neat interfaces show considerable intensity in the OH stretch region suggesting there is already alignment of the interfacial OH oscillators, which would create a local electric field within the interfacial region. Addition of charge via added salt can have one of two effects. It can either weaken the already present field by screening, thereby decreasing the OH peak intensity (the case for the CCl_4−$NaCl_{(aq)}$ spectrum in Figure

16), or induce a larger field which acts to increase the VSF spectral intensity (the case for the air−$NaCl_{(aq)}$ spectrum in Figure 16). When all of the above results are viewed together, these studies of different types of interfaces with salts of varying characteristics reveal how complex the interactions are that take place within the small dimensions of interfacial water molecules adjacent to a hydrophobic phase.

We now shift the focus slightly and survey work from our group and other major contributors that have examined the adsorbates themselves, specifically their orientation, structure, and affinity for the oil−water interface. Although any number of modifications to surfactants can be made for the purposes of study, the most basic modifications for developing a picture are in chain length of the hydrophobic tail and variations in the hydrophilic headgroup. Changing either of these two characteristics of the surfactant can have drastic effects on its properties at the interface: its ability to adsorb to the interface, and as discussed in the previous section, its effect on the surrounding solvating molecules.

Most VSFS studies of alkyl surfactant adsorption focus on the CH vibration modes of the surfactant's hydrophobic tails. These modes are most often studied because they can give information regarding the macroscopic conformational order of the monolayer and the average orientation of the tails. For the purposes of the experiments discussed below which require thinking about local symmetry in the molecule, we will momentarily treat the surfactant tails as simple alkane chains and ignore the headgroup. If the backbone of the chain is in an all *trans* configuration, then methylene modes along the backbone will not be VSF active because the chain is locally centrosymmetric and the transition moments of each opposing methylene will cancel out the VSF signal. If however there is a *cis* configuration somewhere in the chain, then there will be a VSF active methylene transition moment at this gauche defect because it will not be in a centrosymmetric environment. For this reason, VSFS is especially sensitive to the conformation of the adsorbed surfactant tails. Different polarization schemes such as ssp and sps can also be used to indicate conformation and orientation of the surfactant at the interface. In parallel with VSFS studies of surfactants at oil−water interfaces, surface tension data can provide much needed information to help flush out a full picture of the interface.

Variations in chain length drastically change a surfactant's ability to adsorb to the oil−water interface as shown by Conboy et al. in a study of a series of alkane−sulfonates where an SO_3 headgroup is attached to a six, eleven, and twelve carbon tail.[102] Of the three surfactants, the sodium hexanesulfonate (HS) is the least surface active, followed by sodium undecanesulfonate (UDS), and then sodium dodecylsulfonate (DDS). The amplitude ratio of the methyl to methylene modes from the VSF spectra was used as an indicator of chain conformation because a change in this ratio indicates a change in the conformational order of the monolayer.[103] As seen in Figure 17 [Figure 17 is mislabeled in the original manuscript, ref 102], HS has the highest amplitude ratio of methyl to methylene modes indicating the lowest number of gauche defects, followed by UDS, then DDS. These findings show that as the chain of the surfactant is lengthened, more gauche defects are possible and conformational order decreases. Conboy et al. also completed a study of a series of surfactants where the headgroup was varied and the chain length was kept constant at 12 carbons.[104] The four surfactants used were sodium dodecylsulfate (SDS), sodium dodecylsulfonate (DDS), dodecyltrimethylammonium chloride (DTAC), and dodecylammonium chloride (DAC). The methyl to methylene amplitude ratio was used to gain an understanding of the tail conformation at the CCl_4–water interface and how this changes with respect to headgroup. As shown in Figure 18, it is found that both DTAC and DAC have larger methyl to methylene ratios than the SDS and DDS, indicating that the cationic surfactant tails possess less gauche defects than the anionic surfactant tails. It is thought that one of the reasons for this may be due to the penetration depth of the cationic headgroup into the aqueous phase leading to a more water solvated tail and thus a reduced tail fluidity.

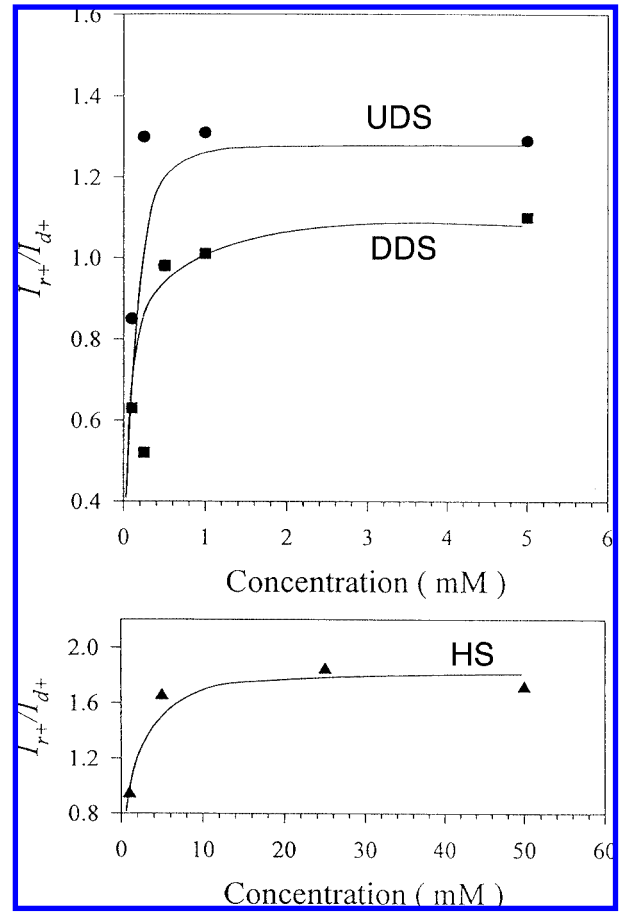

Figure 17. Methyl to methylene ratios for HS, UDS, and DDS, as found from the VSF spectra of the surfactants. Adapted from ref 102.

Continuing with the theme of headgroup variation, Watry and Richmond completed a study of sodium dodecylsulfonate (DDS) and sodium dodecylbenzenesulfonate (DBS) with the difference being a benzene ring located between the SO_3 headgroup and the chain.[105] In these studies Watry et al. found that the addition of the benzene ring to the molecule changes the interfacial properties of the surfactant in a number of different ways. Using the methyl to methylene ratio from the VSF spectra, it was found that the addition of the benzene ring keeps the chains in a disordered state throughout the concentration range up to a full monolayer. Without the benzene ring, changes in the tail conformation are observed with increasing concentration, with a more ordered state existing near full monolayer concentrations. In addition to studying the tails, the first spectra of the high energy CH benzene ring modes at the oil−water interface were published. By probing these CH benzene modes with both ssp and sps polarization schemes, it was found that the benzene ring keeps a vertical orientation throughout the concentration range at the oil−water interface, whereas the benzene ring

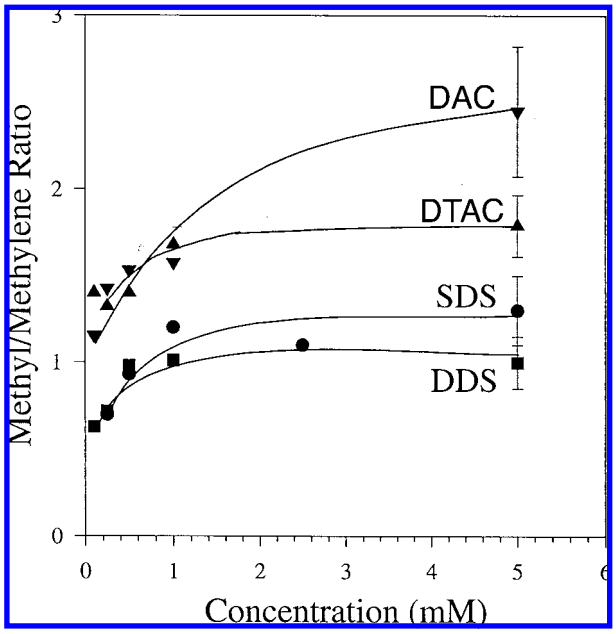

Figure 18. Methyl to methylene ratios for DDS, SDS, DTAC, and DAC, as found from the VSF spectra of the surfactants. Adapted from ref 104.

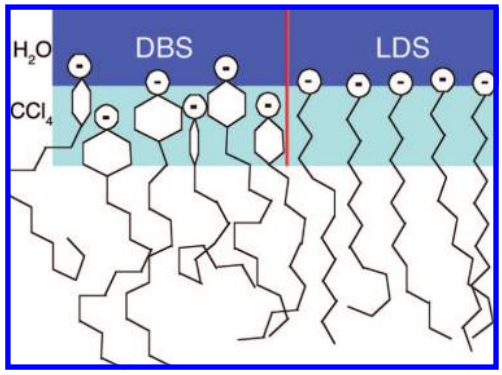

Figure 19. Schematic showing the differences in both the conformation of the tails and the headgroup staggering when DBS (left) and LDS (right) are compared at the CCl_4−water interface

reorients at the air−water interface with respect to concentration. Figure 19 provides a description of these observations. It is also believed that the polarizable nature of the benzene ring leads to a staggered headgroup arrangement at the oil−water interface, which also acts to keep the first few methylenes adjacent to the benzene from interacting with each other, thus leading to disordered chains. Addition of excess NaCl to the surfactant solutions at the air−water interface showed significant increase in the surface activity of the molecules. This is due to screening of the charged sulfate headgroup by excess Na^+, which reduces the Coulombic repulsion between adjacent head groups and thus facilitates a higher degree of packing at the interface. Also in the presence of NaCl, but with the hydrophobic phase changed to CCl_4, the area per molecule at monolayer coverage increases and the bulk concentration at monolayer coverage decreases. This indicates that the surface activity of the molecule is increased due to the screening of charge, but in addition to the excess salt there are also solvent effects to consider. It was concluded that the increased area per molecule is due to the solvation of the chains by the CCl_4, thus more room is required between the chains for the CCl_4 molecules.

Outside of VSFS work by Richmond and co-workers, there have been several other major contributions to the field of surfactants at oil−water interfaces. Bain and co-workers completed an important study of hexadecyltrimethylammonium bromide (CTAB) at the deuterated hexadecane−D_2O interface.[106] This marked the first VSFS study of a surfactant at an alkane-water interface and elucidated some key differences when an alkane is the hydrophobic phase next to water. The importance of the oil phase mixing with the surfactant tails was brought to light and shown to affect the conformation of the surfactant tails, giving rise to a more upright conformation and fewer gauche defects when compared with the air−water interface. This upright conformation occurs at a very sharp transition near monolayer coverage and is unique to this oil–water interface. In addition to VSFS, ellipsometry was used to verify the transition of CTAB to its ordered conformation, giving further evidence of these interesting findings.

Schlossman and co-workers have spearheaded X-ray scattering experiments of surfactants at the alkane−water interface. Their work includes chain length and temperature studies of long chain alcohols adsorbed to both the air−water and hexane−water interfaces, allowing them to gain an understanding of phase changes and the molecular ordering at these two different interfaces.[107,108] It was found that triacontanol ($CH_3(CH_2)_{29}OH$) forms a much more ordered and rigid monolayer at the air−water interface than at the hexane−water interface where the tails have greater fluidity. Adjacent to the headgroup the tails were found to have some structure, but as one moved away from the headgroup, the tails become more disordered into a liquid like regime. It was also found that hexane molecules are interstitially present near the headgroup region, but not as much near the terminal end of the tails, lending to the reason for structure near the headgroup but not at the tail region. The findings of the long chain alcohol studies are interesting in that they are opposite of the findings on CTAB ordering at the air−water versus oil−water interface by Bain and co-workers. This indicates that surfactant properties and adsorption are complex in nature and cannot necessarily be confined to a few simple trends. Schlossman and co-workers have also completed studies of long chain carboxylic acids at the hexane−water interface.[109] The study compared a carboxylic acid headgroup to an alcohol headgroup, with each molecule containing 30 carbons. It showed that the addition of the extra oxygen to the headgroup acts to strongly orient the tails of the surfactant and is attributed to a strong increase in hydrogen bonding between adjacent carboxylic acid head groups. The work is also well supported by their MD results of the same interface.

Oil−water interfaces are important as a model system for studying biologically relevant molecules and processes such as ion transport, membrane formation, and protein folding. A number of studies have investigated the molecular structure of simpler biomolecules at the oil−water interface as a prelude to larger systems. Studies of symmetric phospholipids at the CCl_4−water interface were undertaken by Walker et al. to elucidate the effects of chain length on the conformation of the phospholipid monolayers.[110,111] It was found from the VSF data that the C_3 axis of the terminal methyl group was normal to the interface, which contrasts with data from phosphatidylcholines at the air−solid interface where the terminal methyl was found to have a tilt angle with respect to surface normal.[112] It was also found that shorter chain length phosphatidylcholines packed more efficiently than their longer chain counterparts. The study concludes that CCl_4 more easily solvates longer alkyl chains, which leads to a reduction in the chain−chain interactions and allows for more defects to occur in the monolayer. The chain

length ordering trend at the CCl_4−water interface contrasts with air−water data where the longer chains are not screened from each other by solvent and thus experience stronger van der Waals forces leading to more ordered monolayers. Smiley and Richmond completed a study of asymmetric phosphatidylcholines at the CCl_4−water interface.[113] They found the highly asymmetric phospholipids had increased conformational disorder within the monolayer. This was attributed to the lack of chain−chain interactions due to the largely different chain lengths present on each molecule. Watry and Richmond used VSFS to study a set of important amino acids at the CCl_4−water interface.[114] It was found that each of the amino acids in the study packs loosely with >100 Å^2 per molecule. In addition, it was also found that amino acids with hydrophobic side chains packed much more efficiently than those containing hydrophilic side chains.

From the various studies of biologically relevant molecules, surfactants, and ions at the oil−water interface, it becomes apparent that this unique interface cannot be treated as a simple extension or approximation of the air−water or solid−liquid interface, but rather it needs to be treated and studied as its own unique system.

5. Future Prospects

Liquid interfaces have played a key role in the history of life on earth, both biologically, and now more recently, industrially and scientifically. The importance of the interfacial region has not escaped attention, and it is not surprising that humans have a voracious interest in both understanding and exploiting this unique interface to our advantage. On a fundamental level, there exists a distinct contrast between the interface's simplicity when visually inspected, and simultaneously its complexity on the microscopic scale of molecular structure and in the dynamic hydrogen bonding environment.

There are many exciting opportunities for the future of synthetic chemistry at interfaces. Chemists have long known that water next to a hydrophobic interface can play an invaluable role in both nature and in the laboratory. In the late 1940s, the Diels−Alder reaction was found to be more efficient if conducted "in" water.[115] Forty years later, a rapidly growing interest in green chemistry has spurred research on the use of water as a universal and more environmentally benign solvent in chemical synthesis.[116] This growing interest has also led to the increasing need for a deeper understanding of the complex and unique hydrogen-bonding environments found when an aqueous solution is placed next to a hydrophobic interface. Recent organic synthesis work by Sharpless and co-workers has exemplified the exciting possibilities afforded by organic reactions taking place in emulsions with water (or "on water" as Sharpless says), so as to maximize the amount of interfacial area between water and the organic phase.[117] The unique properties of the emulsion's interfacial region can result in some reactions proceeding as much as 200 times faster than in organic solvents. The mechanisms behind the enhancements in reaction dynamics are the subject of recent work by Marcus and co-workers in which catalysis thermodynamics related to OH bonding is explored.[118] They showed that these astonishing reaction enhancements were the result of prolonged transition states, which were due to molecular complexing of surface water molecules, specifically the free OH, with the transition state molecule.

On another forefront, the liquid−liquid interface has potential in the nanoscience area. Research by Russell and co-workers and Rao and co-workers has pushed the forefront of self-assembly of nanoparticle arrays at the oil−water interface.[119−121] This field is particularly intriguing as the constituents may be biological or synthetic in nature because the oil−water interface seems to be an equal opportunity host. It is also exciting because it represents a broader category of efforts that might be characterized as developing new materials using complex growth conditions. Sometimes appropriate complex conditions must be generated artificially, but in the case of the oil−water interface they exist naturally and thus provide a unique environment for self-assembly.

The liquid−liquid interface will continue to serve as an idealized model system as well. Recent work in this laboratory and elsewhere on the addition of simple ions and larger charged moieties to the oil−water interface means that it will become an even more realistic and attractive system for those that seek to understand the intricacies in fields ranging from atmospheric chemistry to electrochemistry to membrane science.

What is key to future progress in any of these fields, applied or fundamental, will be an ever deepening, deep seated knowledge of both bonding structure and dynamics of the oil−water interface that paces ahead of, and guides investigators in, their quest for new uses for these fluid interfaces. Knowledge such as this, whether it comes from experiment, theory, computation, or a combination of all, will enhance the ability, for example, to predict reactivity at these interfaces or optimize conditions for the best yields. Enabling this continuing drive to understand the fundamentals of the interface will be advances in experimental technique combined with novel approaches in computational and simulation studies. As our recent work attests, when the distinct realms of experiment and simulation/computation are brought together the results are a nonlinear increase in understanding.

Acknowledgment. The authors thank the National Science Foundation (Grant CHE-0652531) for support of this research. Funding from the Office of Naval Research assisted in instrumentation and computational studies.

References and Notes

(1) Ball, P. *Nature* **2008**, *452*, 291–292.
(2) Tanford, C. *Ben Franklin stilled the waves: an informal history of pouring oil on water with reflections on the ups and downs of scientific life in general*; Oxford University Press: New York, 2004.
(3) Pratt, L. R.; Chandler, D. *J. Chem. Phys.* **1977**, *67*, 3683–3704.
(4) Chandler, D. *Nature* **2005**, *437*, 640–647.
(5) Chandler, D. *Nature* **2007**, *445*, 831–832.
(6) Benjamin, I. *J. Chem. Phys.* **1992**, *97*, 1432–1445.
(7) Buhn, J. B.; Bopp, P. A.; Hampe, M. J. *Fluid Phase Equilib.* **2004**, *224*, 221–230.
(8) Conrad, M. P.; Strauss, H. L. *Biophys. J.* **1985**, *48*, 117–124.
(9) Frank, S.; Schmickler, W. *J. Electroanal. Chem.* **2004**, *564*, 239–243.
(10) Geysermans, P.; Elyeznasni, N.; Russier, V. *J. Chem. Phys.* **2005**, *123*, 204711−1204711−8.
(11) Huang, D. M.; Geissler, P. L.; Chandler, D. *J. Phys. Chem. B* **2001**, *105*, 6704–6709.
(12) Hummer, G.; Garde, S.; Garcia, A. E.; Pratt, L. R. *Chem. Phys.* **2000**, *258*, 349–370.
(13) Lee, S. H.; Rossky, P. J. *J. Chem. Phys.* **1994**, *100*, 3334–3345.
(14) Luzar, A.; Svetina, S.; Zeks, B. *Chem. Phys. Lett.* **1983**, *96*, 485–490.
(15) Patel, S. A.; Brooks, C. L. *J. Chem. Phys.* **2006**, *124*, 204706−1204706−14.
(16) Rajamani, S.; Truskett, T. M.; Garde, S. *Proc. Nat. Acad. Sci. U.S.A.* **2005**, *102*, 9475–9480.
(17) Sokhan, V. P.; Tildesley, D. J. *Mol. Phys.* **1997**, *92*, 625–640.
(18) Townsend, R. M.; Rice, S. A. *J. Chem. Phys.* **1991**, *94*, 2207–2218.
(19) Wang, H. B.; Carlson, E.; Henderson, D.; Rowley, R. L. *Mol. Simulat.* **2003**, *29*, 777–785.
(20) Weeks, J. D. *J. Chem. Phys.* **1977**, *67*, 3106–3121.

(21) Wilson, M. A.; Pohorille, A.; Pratt, L. R. *J. Phys. Chem.* **1987**, *91*, 4873–4878.
(22) Tanford, C. *Protein Sci.* **1997**, *6*, 1358–1366.
(23) Ihde, A. J.; Kieffer, W. F. *Selected readings in the history of chemistry*; Division of Chemical Education American Chemical Society: Easton, PA, 1965.
(24) Girault, H.; Kornyshev, A. A.; Monroe, C. W.; Urbakh, M. *J. Phys.: Condens. Matter* **2007**, *19*, 370301.
(25) Reymond, F.; Fermin, D.; Lee, H. J.; Girault, H. H. *Electrochim. Acta* **2000**, *45*, 2647–2662.
(26) Teegarden, D. *Polymer chemistry: Introduction to an Indispensable Science*; National Science Teachers Association Press: Arlington, VA, 2004.
(27) Bachar, M.; Becker, O. M. *J. Chem. Phys.* **1999**, *111*, 8672–8685.
(28) Gawrisch, K.; Ruston, D.; Zimmerberg, J.; Parsegian, V. A.; Rand, R. P.; Fuller, N. *Biophys. J.* **1992**, *61*, 1213–1223.
(29) Jungwirth, P.; Winter, B. *Annu. Rev. Phys. Chem.* **2008**, *59*, 343–366.
(30) Marrink, S. J.; Tieleman, D. P.; van Buuren, A. R.; Berendsen, H. J. C. *Faraday Discuss.* **1996**, 191–201.
(31) Simons, K.; Vaz, W. L. C. *Annu. Rev. Biophys. Biomol. Struct.* **2004**, *33*, 269–295.
(32) Slater, S. J.; Ho, C.; Taddeo, F. J.; Kelly, M. B.; Stubbs, C. D. *Biochemistry* **1993**, *32*, 3714–3721.
(33) Shen, Y. R. *Nature* **1989**, *337*, 519–525.
(34) Conboy, J. C.; Daschbach, J. L.; Richmond, G. L. *Appl. Phys. A: Mater. Sci. Process.* **1994**, *59*, 623–629.
(35) Grubb, S. G.; Kim, M. W.; Rasing, T.; Shen, Y. R. *Langmuir* **1988**, *4*, 452–454.
(36) McArthur, E. A.; Eisenthal, K. B. *J. Am. Chem. Soc.* **2006**, *128*, 1068–1069.
(37) Steel, W. H.; Walker, R. A. *Nature* **2003**, *424*, 296–299.
(38) Steel, W. H.; Walker, R. A. *J. Am. Chem. Soc.* **2003**, *125*, 1132–1133.
(39) Luo, G. M.; Malkova, S.; Yoon, J.; Schultz, D. G.; Lin, B. H.; Meron, M.; Benjamin, I.; Vanysek, P.; Schlossman, M. L. *Science* **2006**, *311*, 216–218.
(40) Luo, G. M.; Malkova, S.; Pingali, S. V.; Schultz, D. G.; Lin, B. H.; Meron, M.; Graber, T. J.; Gebhardt, J.; Vanysek, P.; Schlossman, M. L. *Electrochem. Commun.* **2005**, *7*, 627–630.
(41) Luo, G. M.; Malkova, S.; Yoon, J.; Schultz, D. G.; Lin, B. H.; Meron, M.; Benjamin, I.; Vanysek, P.; Schlossman, M. L. *J. Electroanal. Chem.* **2006**, *593*, 142–158.
(42) Luo, G. M.; Malkova, S.; Pingali, S. V.; Schultz, D. G.; Lin, B. H.; Meron, M.; Benjamin, I.; Vanysek, P.; Schlossman, M. L. *J. Phys. Chem. B* **2006**, *110*, 4527–4530.
(43) Mitrinovic, D. M.; Tikhonov, A. M.; Li, M.; Huang, Z. Q.; Schlossman, M. L. *Phys. Rev. Lett.* **2000**, *85*, 582–585.
(44) Mitrinovic, D. M.; Zhang, Z. J.; Williams, S. M.; Huang, Z. Q.; Schlossman, M. L. *J. Phys. Chem. B* **1999**, *103*, 1779–1782.
(45) Schlossman, M. L. *Curr. Opin. Colloid Interface Sci.* **2002**, *7*, 235–243.
(46) Tikhonov, A. M.; Mitrinovic, D. M.; Li, M.; Huang, Z. Q.; Schlossman, M. L. *J. Phys. Chem. B* **2000**, *104*, 6336–6339.
(47) Bowers, J.; Zarbakhsh, A.; Webster, J. R. P.; Hutchings, L. R.; Richards, R. W. *Langmuir* **2001**, *17*, 140–145.
(48) Doshi, D. A.; Watkins, E. B.; Israelachvili, J. N.; Majewski, J. *Proc. Nat. Acad. Sci. U.S.A.* **2005**, *102*, 9458–9462.
(49) Lee, L. T.; Langevin, D.; Farnoux, B. *Phys. Rev. Lett.* **1991**, *67*, 2678–2681.
(50) Benjamins, J. W.; Jonsson, B.; Thuresson, K.; Nylander, T. *Langmuir* **2002**, *18*, 6437–6444.
(51) Fujiyoshi, S.; Ishibashi, T.; Onishi, H. *J. Phys. Chem. B* **2006**, *110*, 9571–9578.
(52) Benjamin, I. *J. Phys. Chem. B* **2005**, *109*, 13711–13715.
(53) Chang, T. M.; Dang, L. X. *J. Chem. Phys.* **1996**, *104*, 6772–6783.
(54) Morita, A.; Hynes, J. T. *Chem. Phys.* **2000**, *258*, 371–390.
(55) Boyd, R. W. *Nonlinear optics*, 2nd ed.; Academic Press: San Diego, CA, 2003.
(56) Lambert, A. G.; Davies, P. B.; Neivandt, D. J. *Appl. Spectrosc. Rev.* **2005**, *40*, 103–145.
(57) McGilp, J. F. *J. Phys. D: Appl. Phys.* **1996**, *29*, 1812–1821.
(58) Shen, Y. R. *Principles of nonlinear optics*; John Wiley and Sons: New York, 1984.
(59) Zhu, X. D.; Suhr, H.; Shen, Y. R. *Phys. Rev. B: Condens. Matter* **1987**, *35*, 3047–3050.
(60) Allen, H. C.; Raymond, E. A.; Richmond, G. L. *J. Phys. Chem. A* **2001**, *105*, 1649–1655.
(61) Gragson, D. E.; McCarty, B. M.; Richmond, G. L.; Alavi, D. S. *J. Opt. Soc. Am. B: Opt. Phys.* **1996**, *13*, 2075–2083.
(62) McFearin, C. L.; Richmond, G. L. *J. Mol. Liq.* **2007**, *136*, 221–226.
(63) Scatena, L. F.; Richmond, G. L. *J. Phys. Chem. B* **2001**, *105*, 11240–11250.
(64) Bain, C. D.; Davies, P. B.; Ong, T. H.; Ward, R. N.; Brown, M. A. *Langmuir* **1991**, *7*, 1563–1566.
(65) Ji, N.; Ostroverkhov, V.; Tian, C. S.; Shen, Y. R *Phys. Rev. Lett.* **2008**, *1*, 096102−1−096102−4.
(66) Raymond, E. A.; Tarbuck, T. L.; Brown, M. G.; Richmond, G. L. *J. Phys. Chem. B* **2003**, *107*, 546–556.
(67) Scatena, L. F.; Brown, M. G.; Richmond, G. L. *Science* **2001**, *292*, 908–12.
(68) Jeffrey, G. A. *An introduction to hydrogen bonding*; Oxford University Press: New York, 1997.
(69) Richmond, G. L. *Annu. Rev. Phys. Chem.* **2001**, *52*, 357–389.
(70) Gragson, D. E.; Richmond, G. L. *J. Phys. Chem. B* **1998**, *102*, 3847–3861.
(71) Auer, B.; Skinner, J. L. *J. Chem. Phys.* **2008**, In Press,
(72) Buch, V.; Tarbuck, T.; Richmond, G. L.; Groenzin, H.; Li, I.; Shultz, M. J. *J. Chem. Phys.* **2007**, *127*, 204710−1204710−15.
(73) Brown, M. G.; Walker, D. S.; Raymond, E. A.; Richmond, G. L. *J. Phys. Chem. B* **2003**, *107*, 237.
(74) Walker, D. S.; Richmond, G. L. *J. Am. Chem. Soc.* **2007**, *129*, 9446–9451.
(75) Walker, D. S.; Moore, F. G.; Richmond, G. L. *J. Phys. Chem. C* **2007**, *111*, 6103–6112.
(76) Walker, D. S.; Richmond, G. L. *J. Phys. Chem. C* **2008**, *112*, 201–209.
(77) Walker, D. S.; Hore, D. K.; Richmond, G. L. *J. Phys. Chem. C* **2006**, *110*, 20451–20459.
(78) Case, D. A.; et al. *AMBER 7*; University of California: San Francisco, CA, 2002.
(79) Jedlovszky, P.; Vincze, A.; Horvai, G. *J. Mol. Liq.* **2004**, *109*, 99–108.
(80) Jedlovszky, P.; Vincze, A.; Horvai, G. *Phys. Chem. Chem. Phys.* **2004**, *6*, 1874–1879.
(81) Walker, D. S.; Brown, M. G.; McFearin, C. L.; Richmond, G. L. *J. Phys. Chem. B* **2004**, *108*, 2111–2114.
(82) Hore, D. K.; Walker, D. S.; Richmond, G. L. *J. Am. Chem. Soc.* **2008**, *130*, 1800–1801.
(83) Wang, H. F.; Borguet, E.; Eisenthal, K. B. *J. Phys. Chem. B* **1998**, *102*, 4927–4932.
(84) Hore, D. K.; Walker, D. S.; MacKinnon, L.; Richmond, G. L. *J. Phys. Chem. C* **2007**, *111*, 8832–8842.
(85) Hore, D. K.; Walker, D. S.; Richmond, G. L. *J. Am. Chem. Soc.* **2007**, *129*, 752–753.
(86) Gragson, D. E.; Richmond, G. L. *J. Am. Chem. Soc.* **1998**, *120*, 366–375.
(87) Gragson, D. E.; Richmond, G. L. *J. Phys. Chem. B* **1998**, *102*, 569–576.
(88) Schweighofer, K. J.; Essmann, U.; Berkowitz, M. *J. Phys. Chem. B* **1997**, *101*, 10775–10780.
(89) Schweighofer, K. J.; Essmann, E.; Berkowitz, M. *J. Phys. Chem. B* **1997**, *101*, 3793–3799.
(90) Scatena, L. F.; Richmond, G. L. *J. Phys. Chem. B* **2004**, *108*, 12518–12528.
(91) Scatena, L. F.; Richmond, G. L. *Chem. Phys. Lett.* **2004**, *383*, 491–495.
(92) Chang, T. M.; Dang, L. X. *Chem. Rev.* **2006**, *106*, 1305–1322.
(93) Jungwirth, P.; Tobias, D. J. *Chem. Rev.* **2006**, *106*, 1259–1281.
(94) Petersen, P. B.; Saykally, R. J. *Annu. Rev. Phys. Chem.* **2006**, *57*, 333–364.
(95) Wick, C.; Dang, L. X *J. Chem. Phys.* **2007**, *126*, 134702−1134702−4.
(96) Wick, C. D.; Dang, L. X. *J. Phys. Chem. C* **2008**, *112*, 647–649.
(97) Wick, C. D.; Dang, L. X. *Chem. Phys. Lett.* **2008**, *458*, 1–5.
(98) Raymond, E. A.; Richmond, G. L. *J. Phys. Chem. B* **2004**, *108*, 5051–5059.
(99) Chen, X.; Yang, T.; Kataoka, S.; Cremer, P. S. *J. Am. Chem. Soc.* **2007**, *129*, 12272–12279.
(100) Gurau, M. C.; Lim, S. M.; Castellana, E. T.; Albertorio, F.; Kataoka, S.; Cremer, P. S. *J. Am. Chem. Soc.* **2004**, *126*, 10522–10523.
(101) Hofmeister, F. *Arch. Exp. Pathol. Pharmakol.* **1888**, *24*, 247–260.
(102) Conboy, J. C.; Messmer, M. C.; Richmond, G. L. *Langmuir* **1998**, *14*, 6722–6727.
(103) Conboy, J. C.; Messmer, M. C.; Richmond, G. L. *J. Phys. Chem.* **1996**, *100*, 7617–7622.
(104) Conboy, J. C.; Messmer, M. C.; Richmond, G. L. *J. Phys. Chem. B* **1997**, *101*, 6724–6733.
(105) Watry, M. R.; Richmond, G. L. *J. Am. Chem. Soc.* **2000**, *122*, 875–883.
(106) Knock, M. M.; Bell, G. R.; Hill, E. K.; Turner, H. J.; Bain, C. D. *J. Phys. Chem. B* **2003**, *107*, 10801–10814.
(107) Tikhonov, A. M.; Schlossman, M. L. *J. Phys. Chem. B* **2003**, *107*, 3344–3347.

(108) Tikhonov, A. M.; Pingali, S. V.; Schlossman, M. L. *J. Chem. Phys.* **2004**, *120*, 11822–11838.

(109) Tikhonov, A. M.; Patel, H.; Garde, S.; Schlossman, M. L. *J. Phys. Chem. B* **2006**, *110*, 19093–19096.

(110) Walker, R. A.; Conboy, J. C.; Richmond, G. L. *Langmuir* **1997**, *13*, 3070–3073.

(111) Walker, R. A.; Gruetzmacher, J. A.; Richmond, G. L. *J. Am. Chem. Soc.* **1998**, *120*, 6991–7003.

(112) Porter, M. D.; Bright, T. B.; Allara, D. L.; Chidsey, C. E. D. *J. Am. Chem. Soc.* **1987**, *109*, 3559–3569.

(113) Smiley, B. L.; Richmond, G. L. *J. Phys. Chem. B* **1999**, *103*, 653–659.

(114) Watry, M. R.; Richmond, G. L. *J. Phys. Chem. B* **2002**, *106*, 12517–12523.

(115) Woodward, R. B.; Baer, H. *J. Am. Chem. Soc.* **1948**, *70*, 1161–1166.

(116) Otto, S.; Engberts, J. B. F. N. *Pure Appl. Chem.* **2000**, *72*, 1365–1372.

(117) Narayan, S.; Muldoon, J.; Finn, M. G.; Fokin, V. V.; Kolb, H. C.; Sharpless, K. B. *Angew. Chem., Int. Ed.* **2005**, *44*, 3275–3279.

(118) Jung, Y.; Marcus, R. A. *J. Am. Chem. Soc.* **2007**, *129*, 5492–5502.

(119) Lin, Y.; Skaff, H.; Emrick, T.; Dinsmore, A. D.; Russell, T. P. *Science* **2003**, *299*, 226–229.

(120) Lin, Y.; Boker, A.; Skaff, H.; Cookson, D.; Dinsmore, A. D.; Emrick, T.; Russell, T. P. *Langmuir* **2005**, *21*, 191–194.

(121) Rao, C. N. R.; Kalyanikutty, K. P. *Acc. Chem. Res.* **2008**, *41*, 489–499.

JP808212M